C.P. No. 840

C.P. No. 840

MINISTRY OF AVIATION

AERONAUTICAL RESEARCH COUNCIL

CURRENT PAPERS

Comparison of Seven Wing Buffet Boundaries Measured in Wind Tunnels and in Flight

by

D. G. Mabey, M.Sc.(Eng.)

LONDON: HER MAJESTY'S STATIONERY OFFICE

1966

PRICE 11s 6d NET

U.D.C. No. 533.6.013.43 : 533.693

C.P. No.840
September 1964

COMPARISON OF SEVEN WING BUFFET BOUNDARIES MEASURED IN WIND TUNNELS AND IN FLIGHT

by

D. G. Mabey, M.Sc.(Eng.)

SUMMARY

Wing buffet boundaries (for buffet onset) measured on seven wind tunnel models covering an extreme range of planforms are compared with the flight buffet boundaries. The model buffet boundaries are deduced from the variation of fluctuating wing-root strain with incidence at constant Mach number; the flight buffet boundaries are derived from pilot opinion and accelerometer records.

The overall agreement between the tunnel and flight results is fair but there are differences, most of which are probably caused by the low Reynolds number of the tunnel tests. The unsteadiness of slotted tunnels may also influence model buffet over a limited Mach number range.

Future extensions of this dynamic method of buffet measurement on small models are discussed.

Replaces R.A.E. Technical Report No.64013 - A.R.C. 26554

CONTENTS

1 INTRODUCTION

Wing buffet means the wing response, mainly at its fundamental bending frequency, to the random excitation from pressure fluctuations in separated flows[1]. Wing buffet can limit aircraft performance by producing unpleasant vibrations for the aircrew and/or passengers, by disturbing sensitive equipment or even by endangering the structural integrity of the aircraft. Wing buffet often occurs before stalling or longitudinal instability and hence buffet boundaries are as important as stability boundaries.

In flight, buffet boundaries are derived from accelerometers or from pilot opinion. Pilot opinion of buffet severity varies and hence some pilots penetrate further beyond the buffet boundary than others.

In model tests in wind tunnels indications of the types of flow which cause buffeting can be obtained from force measurements, oil flow photographs and trailing-edge pressures[2]. However, buffeting is a dynamic phenomenon and a dynamic measurement is easily obtained on small models[3,4]. The fluctuating wing-root strain (WRS) is measured while incidence increases at constant Mach number (M) and the sudden increase in WRS is taken to indicate buffet onset.

This method has now been used in several British tunnels. Results for seven models presented here show fair agreement between tunnel and flight buffet boundaries although there are differences, most of which are probably caused by the low Reynolds number of the tunnel tests and the tunnel unsteadiness.

2 EXPERIMENTAL DETAILS

On aircraft and wind tunnel models most buffeting is at the lowest symmetric wind bending frequency[3,4] (ω_1). Dynamic similarity between the buffeting of geometrically similar aircraft and models is established when the reduced frequencies $\omega_1 \bar{c}/V$ are comparable. Aircraft and models tested at the same Mach number are tested at nearly the same velocity* so that for dynamic similarity

$$(\bar{c}\ \omega_1)_m/(\bar{c}\ \omega_1)_a \simeq 1 \quad .$$

This relationship is approximately satisfied in the present tests (Table 1) so that the dynamic method of measuring buffet onset is applicable.

---

* V varies with the velocity of sound, which varies with total temperature.

2.1 Buffet measuring equipment

Small recesses are machined in the wing-roots of each model to receive the wing-root strain gauges. The buffet WRS is small ($\varepsilon = 5 \times 10^{-7}$ is typical). Wire gauges were used for the early tests (Models A to C). Semi-conductor gauges were used for the later tests (Models D to G) because of their higher gauge factor (120 for semi-conductor gauges compared to 2 for wire gauges). The temperature sensitivity of semi-conductor gauges does not matter for these tests because tunnel total temperature only varies about $1^{\circ}C$ during the time taken to test at one Mach number. Ideally there are four active gauges, with two gauges on each wing wired to add the port and starboard bending strain signals and thus eliminating the WRS due to model rolling. Table 1 gives details of the bridges used.

Two methods were used to measure the unsteady signal from the strain gauge bridge. The first, used for tests on Models A to D, is shown in a block diagram in Fig.1(a). The WRS bridge is powered by a 6V battery and the signal lead is connected to a switch. The switch leads to a step-up transformer (20/1) and a high gain ($0.5 \times 10^{6}/1$) low noise amplifier.

The amplifier output passes through a thermojunction to a micro-ammeter and is also displayed on an oscilloscope. When a wing is vibrating, owing to flow unsteadiness or buffeting, the amplifier gain is adjusted until a suitable arbitrary reading is obtained on the micro-ammeter (usually about 60 μA) without amplifier "cut-off" showing on the oscilloscope. The switch is then altered so that the oscillator/attenuator signal passes through the transformer. The oscillator frequency is adjusted to approximate to the wing bending frequency and the calibrated attenuator adjusted until the arbitrary reading selected is obtained on the micro-ammeter. The attenuator reading is then proportional to the root-mean square (rms) value of the WRS, i.e.

$$\mu V = k \times (\text{unsteady WRS}) \quad . \qquad (1)$$

The second method, used on Models E to G, is illustrated in Fig.1(b). The WRS bridge is still powered by the 6V battery but the signal lead is connected to a spectrum analyser* which gives a direct voltage reading. The spectrum analyser is first set to measure the total rms signal. Similar results are obtained to those from method 1 so buffet onset is determined. The model is then set about 2° above buffet onset and the signal analysed to find the wing response

---

* A Muirhead 7781 or a Brüel and Kjaer 2107 is suitable.

frequencies. The wing fundamental bending frequency usually provides the largest portion of the signal[3,4] (but see cautionary experience in Ref.5) and is readily apparent. The spectrum analyser is then tuned to the wing fundamental frequency with maximum rejection and the measurements repeated.

Method 1 gives nearly the same value for buffet onset as method 2, but method 2 is quicker and has two other intrinsic advantages:-

(i) the wing fundamental frequency is more easily measured than on an oscilloscope;

(ii) scaling laws[3,4] can be applied when measurements are taken at the wing fundamental frequency. Method 2 is now possible because of the higher signal level of semi-conductor strain gauges compared to wire gauges.

The fluctuating strain gauge signal (μV) is measured, by either method, as incidence (α) increases at constant Mach number. The signal at low incidence is the wing response to tunnel unsteadiness and the increase at higher incidences is caused by wing buffeting. Buffet onset is defined as the intersection of a straight line through the wing response to tunnel unsteadiness and another tangential to the buffet response. This definition is normally precise but a few curves have two sudden changes in slope. For these, the first small change in slope is thought to represent intermittent buffeting induced by the flow unsteadiness just below the buffet boundary; this slope change is ignored. The repeatability of measurement of buffet onset incidence by the means described is usually within about $\pm 0.2^{\circ}$.

The constant k in equation (1) may be deduced from a static calibration but the absolute level of WRS is not required when measuring buffet onset.

2.2 Models

Fig.2 shows the starboard wings of the seven complete scale models of aircraft selected for this comparison of tunnel and flight data. The rear fuselages of Models A to D were a little distorted to accommodate the support stings, but this and other minor differences between the tunnel models and the full scale aircraft should have only small effects on wing buffet.

The tail plane angle on all models was zero relative to the fuselage datum.

2.3 Test conditions

The tunnels and test conditions used are described in Table 1. The low Reynolds number of the initial Model A tests and the Model C tests in the R.A.E. 3 ft tunnel were due to a power limitation.

Transition-fixing bands of carborundum in aluminium paint were attached to the leading edges of the wings, tailplane and fin of every model. Transition was also fixed on every fuselage except on Model B.

3 RESULTS

3.1 Model A

Fig.3 shows the variation of WRS signal with incidence. The incidence for buffet onset (α_B) is sharply defined at M = 0.50 to 0.70 (Fig.3(a)) but rather less clearly defined from M = 0.80 to 0.96 (Fig.3(b)).

Oil flow photographs taken at and near buffet onset show a close association of wing buffeting with flow separation, of course the oil flow shows an average surface flow pattern (Fig.4). At subsonic speeds (Fig.4(a)) the flow below buffet onset is streamwise with some outboard flow towards the trailing egde. At buffet onset the flow separates outboard of the leading edge kink and re-attaches at about 40% chord; downstream of re-attachment there is marked outflow towards the trailing edge. The flow in the small separated flow region is complex. Above buffet onset the wing buffet builds up rapidly (Fig.3(a)) as the separated region quickly extends downstream to the trailing edge and inboard to the root.

At transonic speeds (Fig.4(b)) the flow below buffet onset is streamwise with a little outboard flow towards the trailing edge. At buffet onset a change in curvature of the oil flow streamlines from 50% semi-span to the tip indicates a shock wave which just separates the flow from about 70-80% semi-span. The flow re-attaches however and continues streamwise to the trailing edge. Above buffet onset wing buffet builds up slowly (Fig.3(b)). The separated region quickly extends to the trailing edge and the shock slowly moves forward. The flow near the wing root does not separate although a large spanwise flow develops towards the separated region. Earlier work on unswept wings shows that buffeting starts as the average re-attachment point approaches the trailing-edge (because the re-attachment point reaches the trailing-edge intermittently) and this corresponds with the present buffet onset.

Fig.5 shows a comparison of the buffet boundaries (buffet onset lift coefficients plotted against Mach number) measured in the tunnel and in flight. The tunnel and flight results agree well except at M = 0.80 when the tunnel

results look too low*. The buffet onset in flight was sharply defined so that pilots had no diffioulty in establishing the flight buffet boundary. Pilots liked the aircraft buffeting characteristics because, although buffet onset was sharply defined, the buffeting subsequently increased slowly with incidence. Hence safe penetration above the buffet boundary was possible.

Early tests at a lower Reynolds number ($R = 0.7 \times 10^6$) (imposed by power limitations) gave a higher buffet boundary with a definite break between $M = 0.80$ and 0.81, corresponding with the change from leading-edge to shock induced separations (Fig.6). The agreement with flight results is fair from $M = 0.50$ to 0.80 but poor from $M = 0.81$ to 0.93. In this Mach number range, with shock induced separations, the buffet boundary should be lower than at the higher Reynolds number, as for Models E and F. This anomalous result for Model A is a warning against buffet tests made at very low Reynolds numbers (i.e. less than 1.0×10^6).

Trailing-edge static pressure measurements on Model A are discussed in the Appendix.

3.2 Model B

Fig.7 shows the variation of WRS with incidence for Model B in the R.A.E. 3 ft tunnel. The incidence for buffet onset is well defined except at $M = 0.80$ and 0.82 where there are two sudden changes of slope in the curve (cf. 2.1 above).

Fig.8 shows corresponding data measured in the DH 2 ft tunnel at nearly identical Reynolds numbers. Buffet onset is again sharply defined, except at $M = 0.75$, 0.88 and 0.90.

Fig.9 shows a comparison of the buffet boundaries measured in both tunnels and in flight. Generally, both tunnel curves agree and reproduce the shape of the flight results - even the plateau from $M = 0.70$ to 0.80. However, the tunnel results are fairly consistentely about 0.08 too low in C_L compared with the flight data. This discrepancy may be caused by small differences between the model and the aircraft**, or the large differences in Reynolds number between the tunnel and flight results (1×10^6 compared to 40 to 50×10^6).

---

* An earlier oil flow photograph at $M = 0.80$ showed no separation just above the present tunnel buffet boundary. Transonic leading-edge attachment occurs on this wing at $M = 0.81$ and because this is sensitive to the boundary layer state[9], it is intended to repeat these tests with different grades of roughness at a later date.

** Tests in the DH 2 ft tunnel (July 1963) with small changes to the model rear fuselage give a tunnel buffet boundary about 0.04 higher than in the present tests.

The buffet boundary measured in the 3 ft tunnel from M = 0.82 to 0.88 is lower than both the 2 ft tunnel and the flight buffet boundaries. This premature buffet may be associated with the high level of wing response to the flow unsteadiness in the 3 ft tunnel which is most severe from M = 0.80 to 0.90 (Fig.10).

3.3 Model C

Fig.11 shows the variation of WRS signal with incidence for Model C in the R.A.E. 3 ft tunnel. Buffet onset is sharply defined, except at M = 0.80, 0.93, 0.96 and 0.99. This model was previously tested in the A.R.A. tunnel at higher Reynolds numbers with similar results: here there was no difficulty in defining buffet onset (Fig.12).

Fig.13 shows a comparison of the buffet boundaries measured in both tunnels and in flight. Generally, both tunnel curves agree (apart from the 3 ft tunnel point at M = 0.90) and correspond very well with the flight data, which is only available from M = 0.70 to 0.91.

3.4 Model D

Fig.14 shows the variation of WRS signal with incidence for Model D. Buffet onset is not as sharply defined as on the other models. In flight pilots report that buffet onset is well defined and that buffet severity increases slowly (as on Aircraft A). There is excellent agreement between the tunnel results and the extensive flight data (at altitudes from 5,000 to 30,000 ft) except possibly from M = 0.80 to 0.85. However even in this range the difference between the two mean curves is not much greater than the scatter on the flight data (Fig.15).

One test suggests that the unsteadiness in the slotted working section of the 3 ft tunnel[10] alters the model buffet boundary in the transonic range. The unsteadiness originates in the extraction region at the end of the slotted working section and is reduced by closing the slots. Hence the buffet onset was measured with the slots open and then with the slots closed with Lasevic tape*. When the unsteadiness is small, as at M = 0.60, there is only a small difference between buffet onset with the slots open or closed (Fig.16(a)). When the unsteadiness is severe, as at M = 0.85, buffet onset occurs at an incidence 1.2° lower with the slots open than with the slots closed (Fig.16(b)). The buffet onset measured with the slots closed would improve the tunnel-flight

---

* Reynolds number had to be reduced to prevent the tape tearing.

comparison at M = 0.85 (Fig.15). The slots cannot be closed for the higher Mach numbers (0.90 to 1.00) and another way of reducing the unsteadiness must be found.

3.5 Model E

Fig.17 shows the variation of WRS signal with incidence for Model E. Buffet onset is sharply defined in the tunnel and in flight. Fig.18 shows the tunnel and flight buffet boundaries. The tunnel buffet boundary is much lower than the flight buffet boundary from M = 0.40 to 0.85. Comparison of the flow in this Mach number range on the model[11] and the aircraft[12] reveals a large scale effect on the tip separation favourable to the aircraft. At M = 0.90, when the separations are shock induced, scale effects are smaller and the tunnel and flight results are in closer agreement.

3.6 Model F

Fig.19 shows the variation of WRS signal with incidence for Model F. Although buffet onset is sharply defined, the wing buffet signal is smaller than the tunnel unsteadiness signal (WRS signal at $\alpha = 0^{\circ}$) above M = 0.65. The tunnel unsteadiness is particularly severe in the range from M = 0.80 to 0.93.

Fig.20 shows the tunnel and flight buffet boundaries. The tunnel buffet boundary is much lower than the flight buffet boundary[13] from M = 0.40 to 0.80 because of the large scale effect on the tip separation favourable to the aircraft. This favourable scale effect at M = 0.50 is illustrated by comparing the area of separated flow shown by oil flow* on the model (Fig.21) and by tuft observations in flight (Fig.8, Ref.13). Similar scale effects are noticed on the larger model[13]. Scale effects are smaller when the separations are shock induced and hence the tunnel and flight results are in better agreement from M = 0.85 to 0.96.

The buffet on this aircraft is mild and hence there is even more scatter than usual on the flight data.

3.7 Model G

Fig.22 shows the variation of WRS signal with incidence for Model G. Buffet onset is sharply defined at all Mach numbers, although the curves are different from those of the previous models. Thus the initial signal level

---

* These oil flow photographs also show how slowly the region of separated flow extends with incidence on this highly swept wing compared to the wing with low sweepback (Fig.4(a)).

varies and at some speeds actually decreases just below buffet onset. Above buffet onset, from M = 0.50 to 0.65, the buffet initially builds up rapidly for about 1° beyond buffet onset and then increases more slowly.

In flight buffet never becomes limiting. The buffet onset is not sharply defined and hence a mean curve has been drawn (Fig.23). The pilots merely report first slightly disagreeable buffet and then disagreeable buffet. There is fair agreement between the tunnel and flight boundaries, although the flight buffet boundary looks low at M = 0.70.

4 DISCUSSION

The buffet boundaries measured on Models A to G, covering an extreme range of planforms, show fair overall agreement with flight boundaries, both with regard to the initial level at subsonic speeds and also the subsequent Mach number variation. Although the tunnel results are usually somewhat pessimistic they justify the inclusion of unsteady WRS measurements in any future project model tests. However the present buffet measurements have some limitations.

The most serious limitation is the low test Reynolds number in the present tests in the 3 ft tunnel*. This is only about 1×10^6 for all the models (except Model F); sufficiently low to raise doubts whether full scale separations can be reproduced even with correct boundary layer transition fixing. The recent removal of a power restriction on the tunnel has raised the available Reynolds number to about 2×10^6, which may be high enough to reproduce full scale separations on wings with low to moderate sweepback. Model B may be tested in the future to check this (5.1). On more highly swept wings such as Models E and F, full scale separations may still not be reproduced even at this Reynolds number because scale effects persist on a larger model[13] of the FD 2 (Model F) even at a Reynolds number of 10×10^6.

The other limitation is imposed by unsteadiness in the 3 ft tunnel[10]. The results for Model B (from M = 0.80 to 0.88) and Model D (M = 0.85) clearly show that tunnel unsteadiness can sometimes influence model buffet. The magnitude of this effect varies from model to model but is important only when the unsteadiness signal (WRS signal at $\alpha = 0^{\circ}$) is large compared to the total signal. Elimination of this unsteadiness is a difficult task which may take some time to complete.

---

* This is an acknowledged limitation of measurements made in this tunnel at half power, not a limitation of the technique used to measure model buffet.

This discussion assumes that the flight results may be compared directly with the tunnel data. This assumption may be questioned, because most of the flight data are based on pilot opinion, and pilots can detect buffet only when there is a finite wing vibration. In contrast the tunnel buffet onset corresponds with a vanishingly small wing vibration above the level caused by tunnel unsteadiness. Flight buffet onset boundaries derived from WRS measurements would probably correlate better with the tunnel boundaries. Flight measurements of WRS are needed to establish the correct scaling relationships for buffet loads (5.2).

5 FUTURE DEVELOPMENTS

Future developments of this method of buffet testing are now discussed.

5.1 Roughness height and Reynolds number

An investigation of roughness height and Reynolds number effects on tunnel buffet boundaries may explain some of the present differences between tunnel and flight results.

5.2 Buffet loads

Two problems must be solved to predict full scale buffet loads from model tests. The first problem is the separation of model buffet loads from the loads caused by tunnel unsteadiness; comparative tests on Model B in two tunnels indicate a correlation between model buffet and tunnel unsteadiness near buffet onset. The best solution would, of course, be to ensure a low level of tunnel unsteadiness. If the tunnel unsteadiness is low, the increase of WRS signal above buffet onset indicates the magnitude of model buffet load. Additional measurements and assumptions are required to scale model buffeting to aircraft[3,4]. Rainey has discussed the scaling problem introduced by wing damping in model buffet tests[14]. On Models A, B, D and E measurements at constant Mach number (not presented) indicate that,

$$\varepsilon_B \propto \rho \qquad (2)$$

so that the damping of the motion appears to be predominately structural[15]. This is particularly surprising on Model B where the wings and centre fuselage are machined from one piece of dural and the structural damping should be low. In flight the damping should be mainly aerodynamic so that

$$\varepsilon_B \propto \rho^{\frac{1}{2}} \quad .$$

Until these inconsistencies are explained, extrapolation from model to full scale buffet loads appears impossible.

A recent report[16] presents scaling relationships appropriate for launch vehicles.

5.3 Half models

Half models have some advantages for buffet tests. The Reynolds number may be increased by a factor of $2\frac{1}{2}$ (for the same blockage) as compared with a complete model and unwanted vibration modes of the complete model (pitch, heave and roll) are eliminated. Since overall forces are not required the gap between the half model and the balance can be sealed and thus the leak flow between the wing surfaces eliminated. The side wall boundary layer remains however, and the fuselage must be represented correctly, because this affects both the strength and position of the main shock over the wing, and hence the wing buffet[15].

Fair agreement between the buffet boundary measured in the DH 2 ft tunnel on Model B and on a similar half model has been reported[17,18].

6 CONCLUSIONS

Dynamic wing buffet measurements on seven small models in the 3 ft tunnel suggest four important conclusions.

(i) There is fair correlation between the tunnel and flight buffet boundaries over an extreme range of planforms and thickness distributions. The tunnel results are usually somewhat pessimistic but would still be valuable for project studies.

(ii) A Reynolds number of 1×10^6 is hardly high enough to obtain correct representation of full scale separations and hence full scale buffet, even on wings with low sweepback*.

(iii) Unsteadiness in the 3 ft tunnel is rather high in the range from $M = 0.80$ to 1.00. It may influence model buffet and should be reduced.

(iv) Flight measurements of unsteady WRS are needed for comparison with tunnel measurements and to verify the scaling relationship for buffet loads.

---

* The restoration of full power to the 3 ft tunnel will raise the Reynolds number on typical models from about 1×10^6 to 2×10^6

Appendix

TRAILING-EDGE STATIC PRESSURE DIVERGENCE BOUNDARIES ON MODEL A

Trailing-edge static pressure divergence indicates the threshold of serious separation effects[2]. Trailing-edge divergence boundaries were measured previously (June 1958) at five spanwise stations on Model A and compared to the flight buffet boundary.

Model A has no static pressure holes and so a simple modification was adopted (Fig.24). Five hypodermic tubes were attached to the lower wing surface with araldite and supported on a bracket clamped to the model sting a short distance downstream of the tailplane. Two holes were drilled through every hypodermic tube at the trailing-edge to record the static pressure. The tube spanwise station were

$$2y/b = 0.40, 0.55, 0.69, 0.82, 0.95$$

as on an ARA half model.

Fig. 25 shows the variation of trailing-edge static pressure with lift coefficient for a typical station $2y/b = 0.82$. The onset of separation is fairly sharply defined by the pressure divergence up to $M = 0.93$. There is no divergence at $2y/b = 0.40$ and oil flow photographs show no separation at this station. The present results agree well with the ARA half model measurements.

Fig.26 shows the trailing-edge static pressure divergence boundaries. The measurements at $2y/b = 0.95$ bear no relation to the flight buffet boundary, and are dominated by the tip vortex. The boundary for $2y/b = 0.82$ corresponds very well with the flight results from $M = 0.70$ to 0.90 but not from $M = 0.40$ to 0.70. The trailing-edge divergence boundary ends between $M = 0.93$ and 0.96, where the flow becomes supersonic at the trailing-edge (see Fig.25) whereas the flight buffet boundary rises rapidly from $M = 0.93$ to 0.96.

Trailing-edge pressure measurements are difficult on small 3 ft tunnel models designed for overall force measurements without static pressure holes, for which the dynamic method of buffet measurement is preferred. This method gives a continuous buffet boundary which covers the complete Mach number range from $M = 0.40$ to 0.99.

Tunnel unsteadiness alters shock strengths and shock positions in the transonic region (Fig.5.4, Ref.19) and hence may influence trailing-edge divergence boundaries as well as dynamic buffet boundaries.

Table 1

TEST CONDITIONS

Model	Tunnel	Working section	Reynolds number(s) R	WRS bridge	Wing frequency c/s	$(\omega_1 c)m/(\omega_1 c)a$	Sting support	Date of tests
A	R.A.E. 3 ft	4 sides slotted (Ref.6)	0.7×10^6 1.3×10^6	2 active wire gauges + 2 external resistors	580	1.62	6 component balance	March 1959 March 1960
B	R.A.E. 3 ft	TABS (Ref.7	0.6×10^6 to 0.9×10^6	4 active wire gauges	240	1.05	Solid sting	June 1962
	D.H. 2 ft	TABS (Ref.8)	0.6×10^6 to 0.8×10^6					October 1962
C	R.A.E. 3 ft A.R.A. 8 x 9 ft	TABS (Ref.7) Perforated	0.8×10^6 1.3×10^6	2 active wire gauges + 2 external resistors	-	-	6 component balance	January 1962 October 1960
D	R.A.E. 3 ft	TABS (Ref.7)	1.2×10^6 and 0.9×10^6	4 active semi-conductor gauges	492	1.41	6 component balance	October 1963
E	R.A.E. 3 ft	TABS (Ref.7)	1.0×10^6 and 0.8×10^6	4 active semi-conductor gauges	665	1.15	3 component balance	February 1964
F	R.A.E. 3 ft	TABS (Ref.7)	2.4×10^6 and 1.8×10^6	4 active semi-conductor gauges	323	1.50	6 component balance	February 1964
G	R.A.E. 3 ft	TABS (Ref.7)	1.2×10^6 and 0.9×10^6	4 active semi-conductor gauges	283	0.75	3 component balance	February 1964

TABS ≡ Top and bottom slotted section

SYMBOLS

b	wing span
$\bar{c}$	average chord
C_L	lift coefficient
C_p	pressure coefficient
k	constant (equation 1)
M	Mach number
R	Reynolds number (average chord $\bar{c}$)
y	spanwise distance from model centre line
V	velocity
WRS	wing-root strain
α	incidence
ε	rms strain at wing-root
ρ	density
ω_1	lowest wing bending frequency

Subscripts

B	buffet
f	full-scale
m	model

REFERENCES

No.	Author	Title, etc.
1	R. A. Fail	Unpublished M.O.A. Report
2	H. H. Pearcey	Simple methods for the prediction of wing buffeting resulting from bubble type separation. N.P.L. Aero Report 1024 (A.R.C. 23,884), June 1962
3	W. B. Huston	A study of the correlation between flight and wind tunnel buffet loads. AGARD Report 111 (A.R.C. 20,704), April 1957
4	D. D. Davis W. B. Huston	The use of wind tunnels to predict flight buffet loads. NACA RM L57D25 NACA TIL 5570, June 1957
5	R. H. Landon	Unpublished ARA Report
6	E. P. Sutton M. J. Caiger A. Stanbrook	Performance of the 36 x 35 inch slotted transonic working section of the R.A.E. Bedford 3 ft wind tunnel. (A.R.C. 21,908) R & M 3228, January 1960
7	D. G. Mabey	Calibration of the top and bottom slotted transonic section for the 3 ft tunnel. Unpublished M.O.A. Report
8	J. A. Kirk	Design and operational problems of the transonic jet-driven wind tunnel. Journ. Royal Aero Soc. 62, 6, January 1958
9	D. G. Mabey	Leading-edge attachment in transonic flow with laminar or turbulent boundary layers. Journ. Aero/Space Sci., September 1962 A.R.C. 23123
10	D. G. Mabey	Unpublished M.O.A. Report
11	E. P. Sutton A. Stanbrook	A wind tunnel investigation of the longitudinal stability of the Javelin aircraft at transonic speeds, including a comparison with flight test results. A.R.C. R & M 3403, December 1959
12	D. R. Andrews M. Coxon R. Rose	The development of an artificial stall warning system for a delta wing aircraft (Javelin Mk.1). R.A.E. Report Aero 2579 (A.R.C. 19,356 - S and C 3194) December 1956

REFERENCES (Contd.)

No.	Author	Title, etc.
13	F. W. Dee P. O. Nicholas	Flight determination of wing flow patterns and buffet boundaries for the Fairey Delta 2 aircraft at Mach numbers between 0.4 and 1.3 and comparison with wind tunnel tests. R.A.E. Technical Report No.64012
14	A. G. Rainey T. A. Byrdsong	An examination of methods of buffeting analysis based on experiments with wings of varying stiffness. NASA TN, August 1959
15	D. D. Davis D. E. Wornom	Buffet tests on an attack-airplane model with emphasis on analysis of data from wind tunnel tests. NACA RM L57H13 NASA TIL 6772, February 1958
16	R. V. Doggett P. W. Hanson	An aeroelastic model approach for the prediction of buffet bending loads on launch vehicles. NASA TN D2022 (A.R.C. 25,444), October 1963
17	P. Myers	Unpublished D. H. Wind Tunnel Note 633, July 1963
18	P. Myers	Unpublished D. H. Wind Tunnel Note 646, August 1963
19	B. H. Göethert	Transonic wind tunnel testing. Agardograph No.49, Pergamon Press, 1961

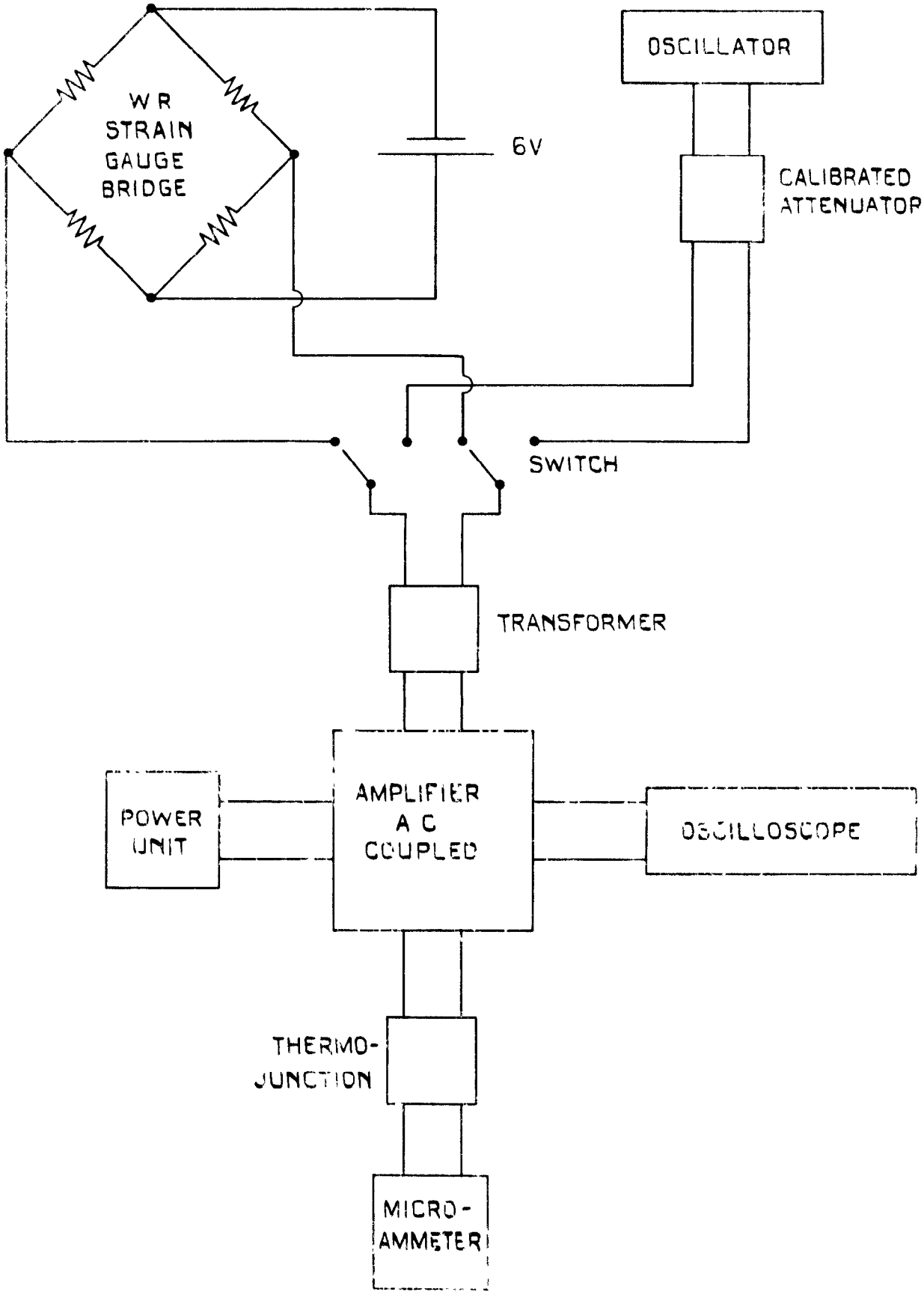

(a) USED ON MODELS A TO D

FIG.1 MODEL BUFFET MEASURING EQUIPMENT

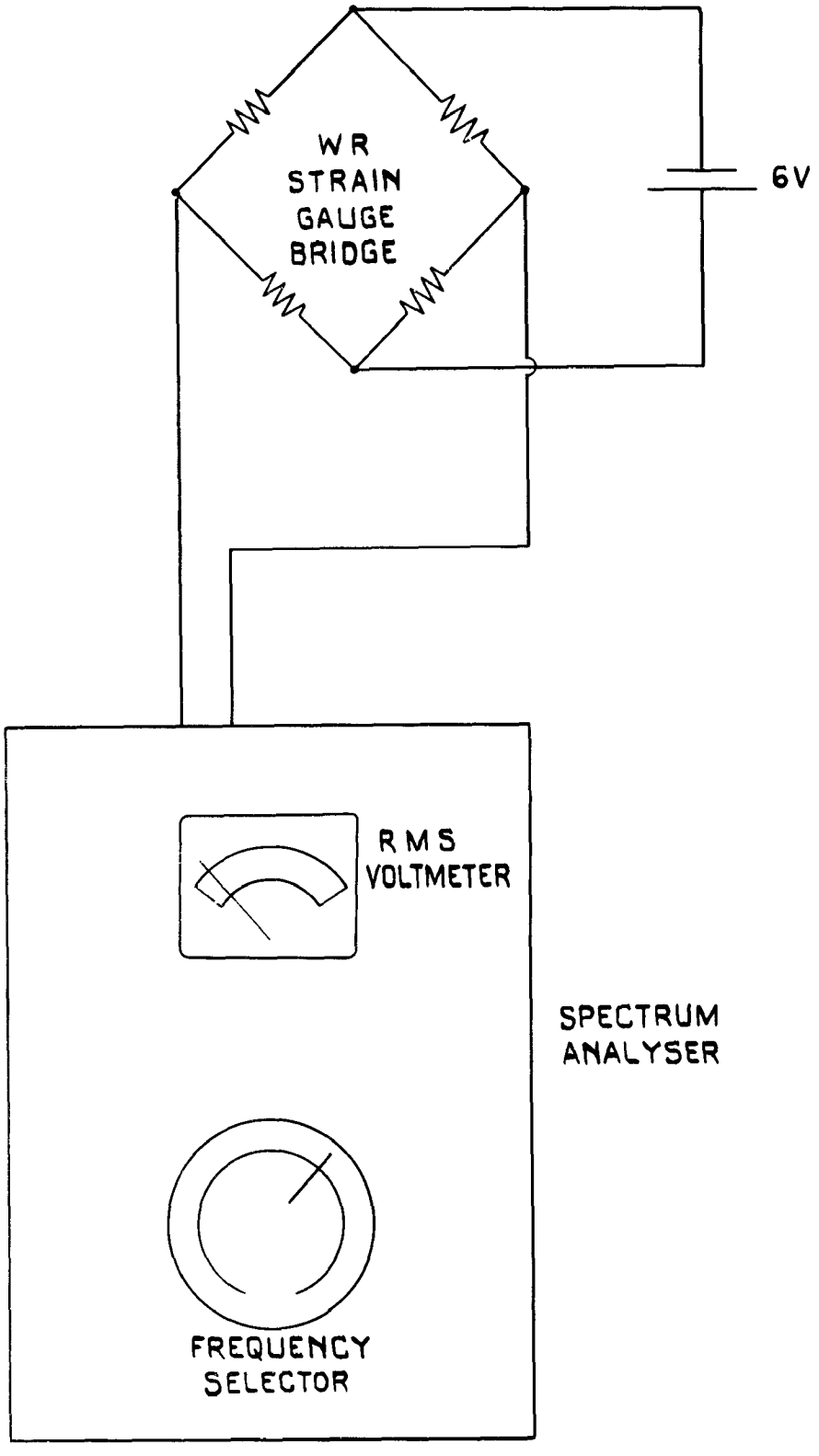

(b) USED ON MODELS E TO G

FIG.1 (CONCLD)

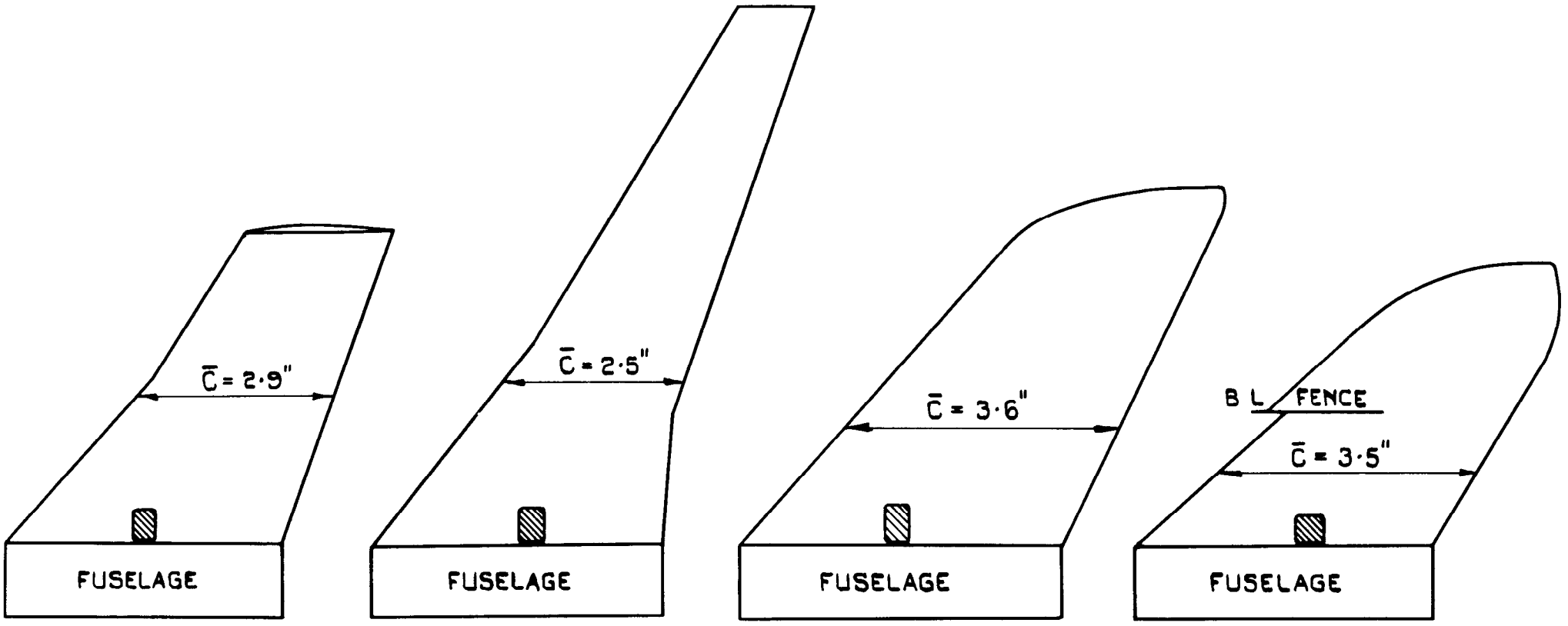

(a) WINGS A TO D

FIG. 2 WINGS TESTED

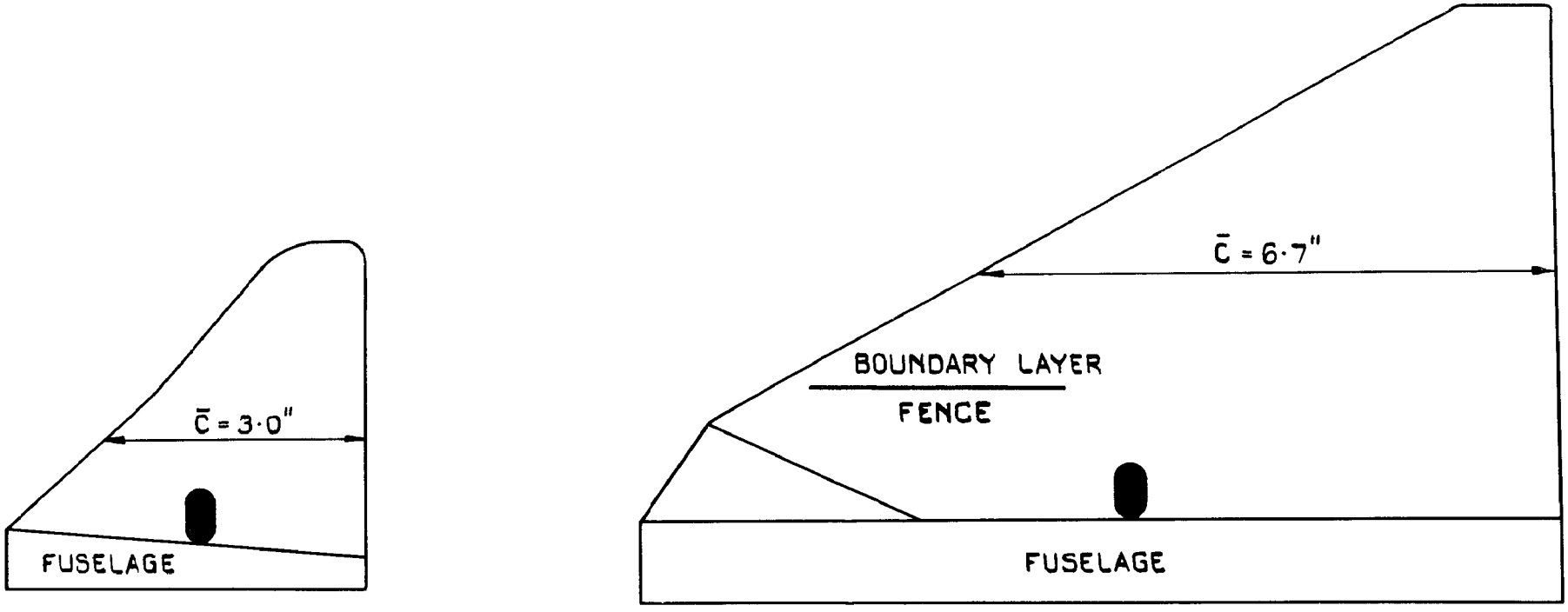

(b) WINGS E AND F

FIG. 2 (CONTD)

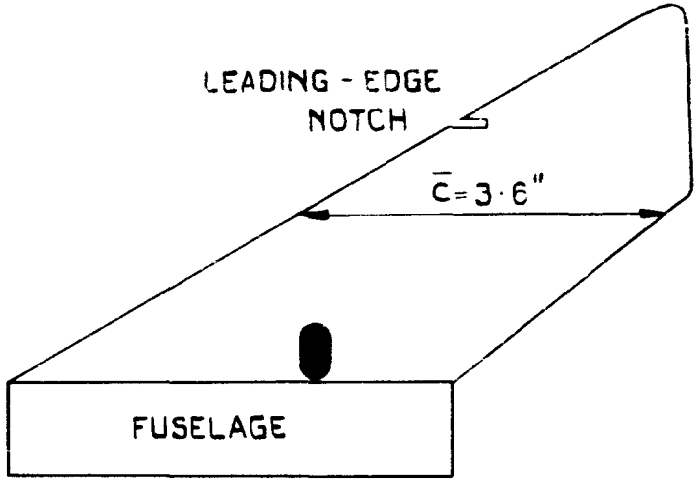

(c) WING G

FIG. 2 (CONCLD)

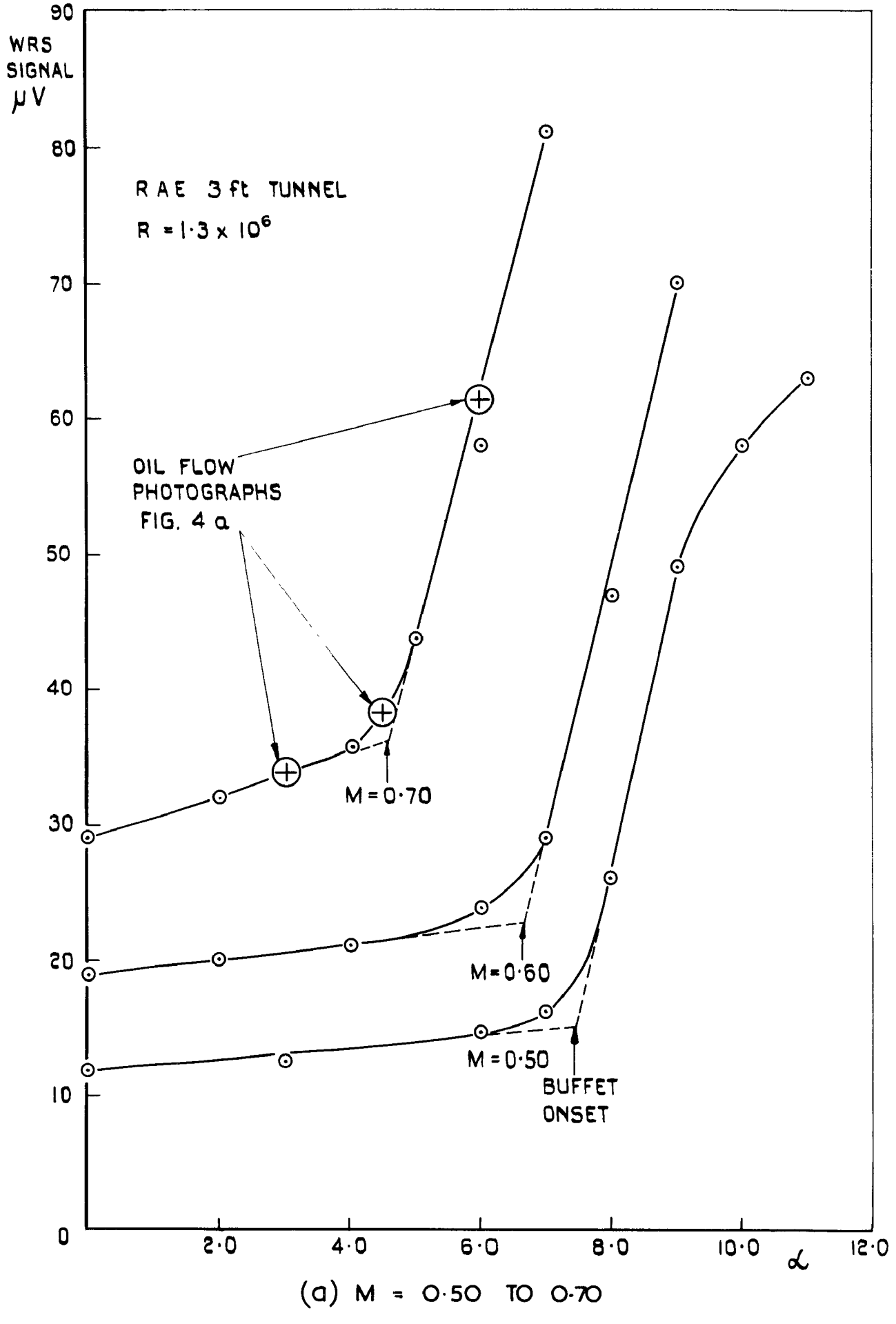

(a) M = 0·50 TO 0·70

FIG. 3 MODEL A - VARIATION OF WING-ROOT STRAIN SIGNAL WITH INCIDENCE.

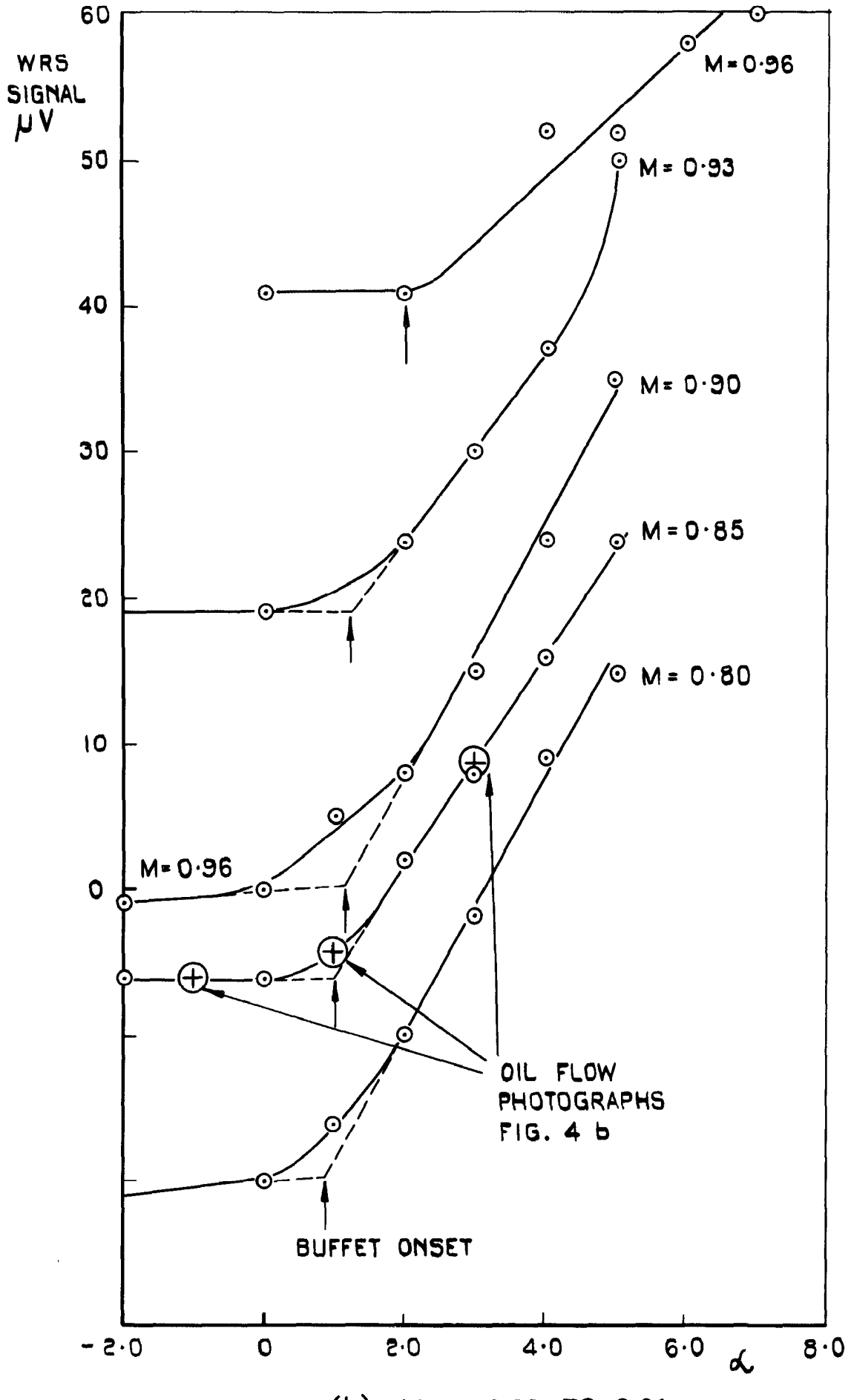

(b) M = 0.80 TO 0.96

FIG. 3 (CONCLD)

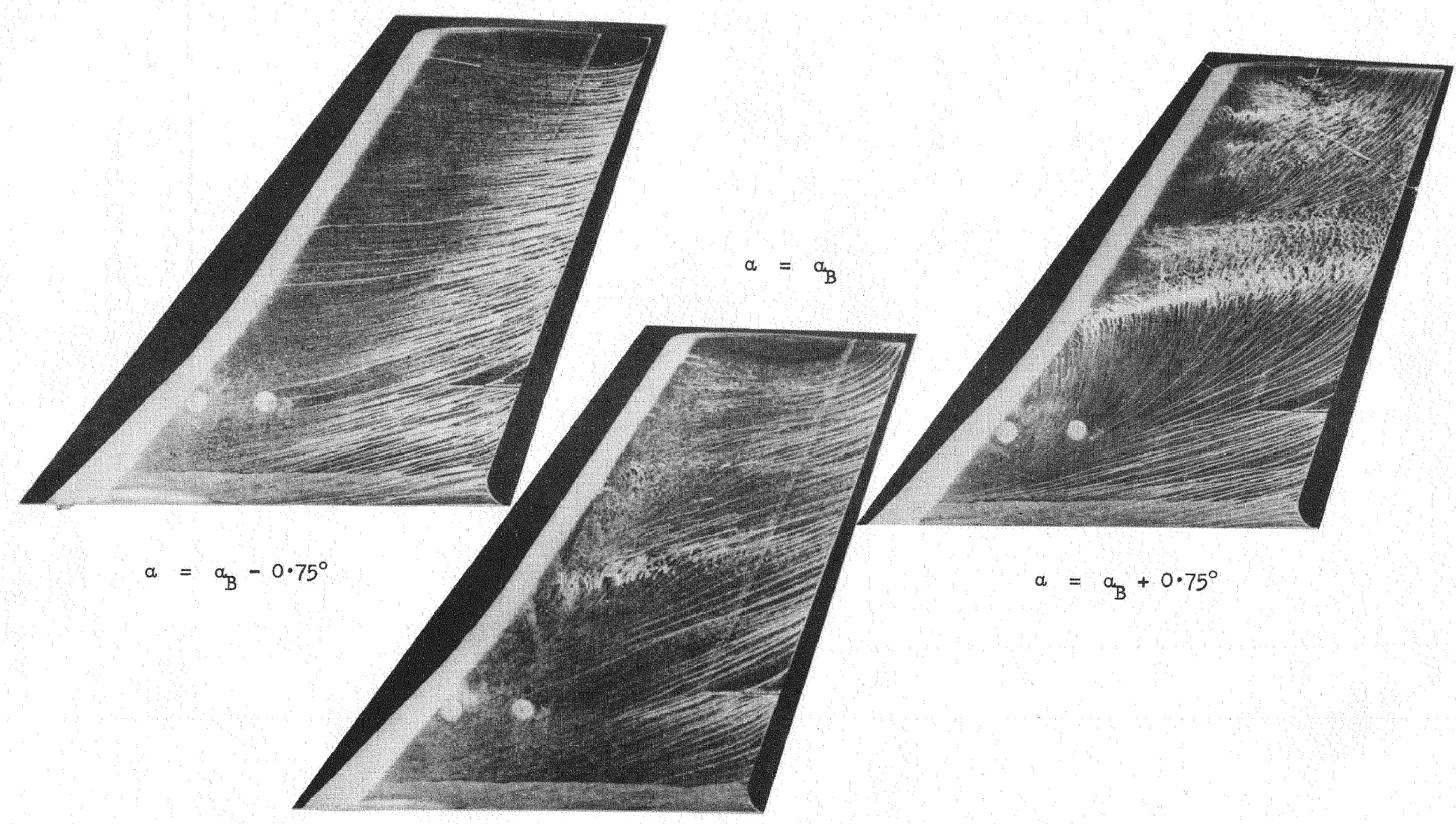

(a) Subsonic M=0·70

Fig. 4. Wing A. oil flow photographs near buffet onset

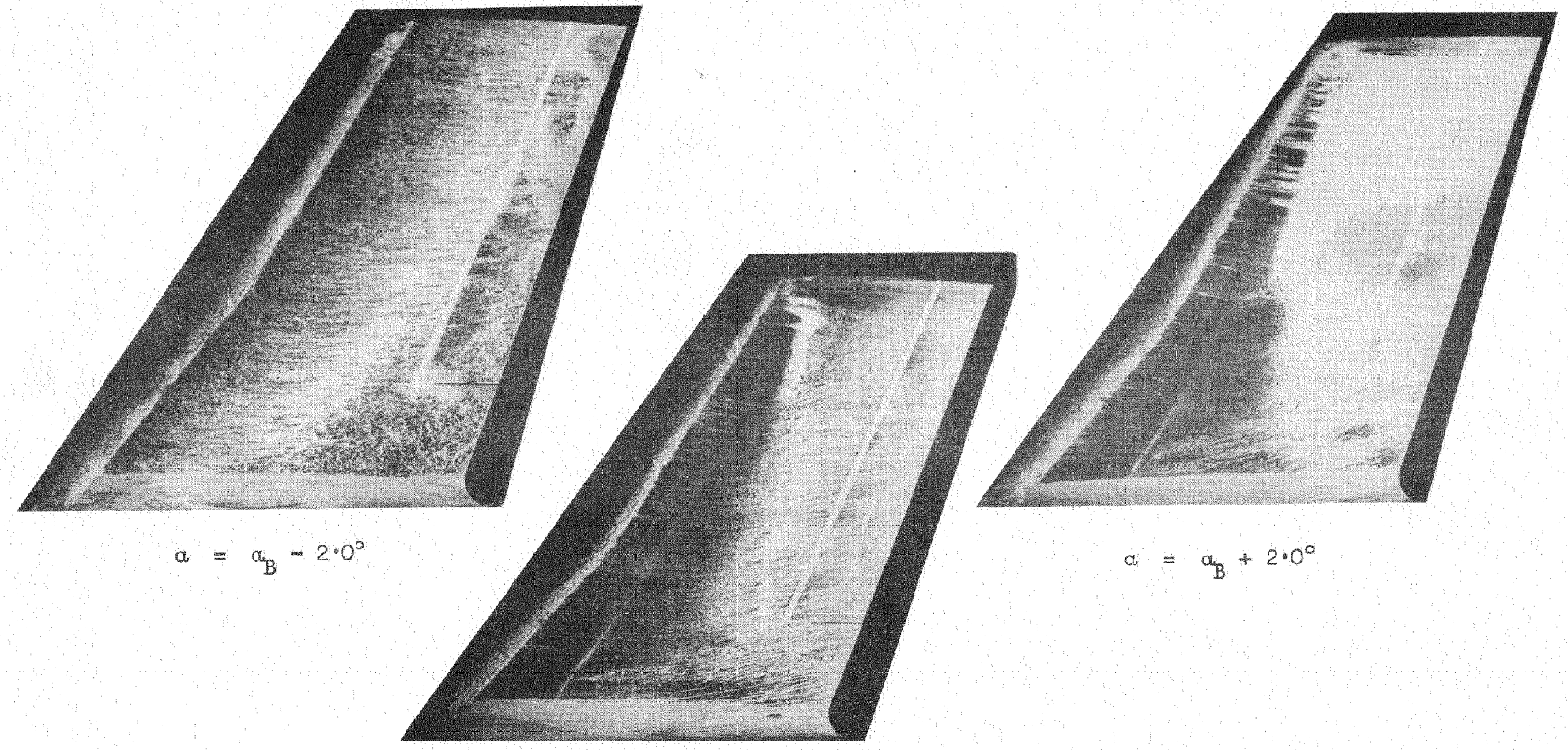

$\alpha = \alpha_B - 2{\cdot}0°$

$\alpha = \alpha_B + 2{\cdot}0°$

Fig. 4. Concl'd .

(b) Transonic M=0·85

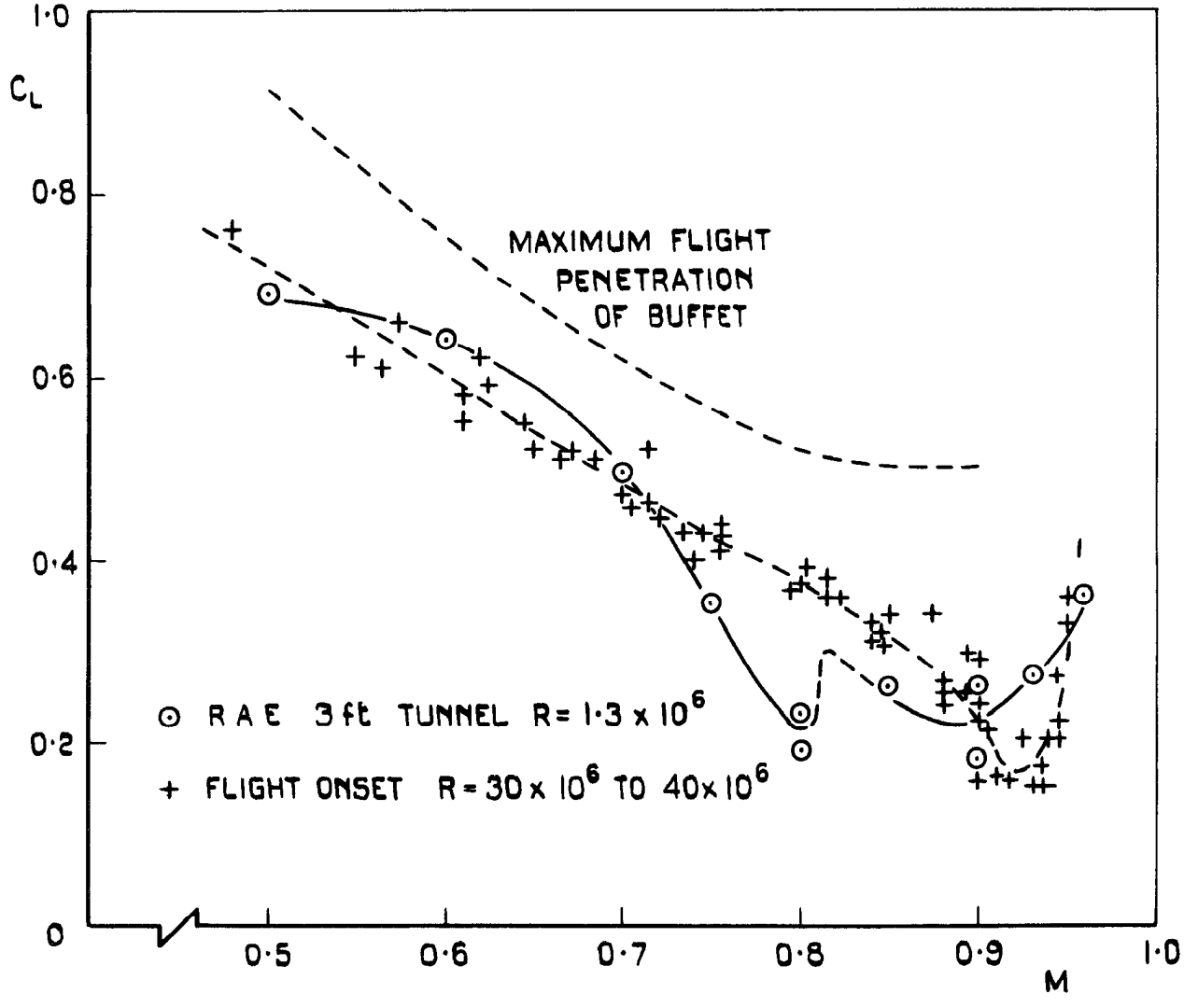

FIG. 5 MODEL A - COMPARISON OF TUNNEL AND FLIGHT BUFFET BOUNDARIES

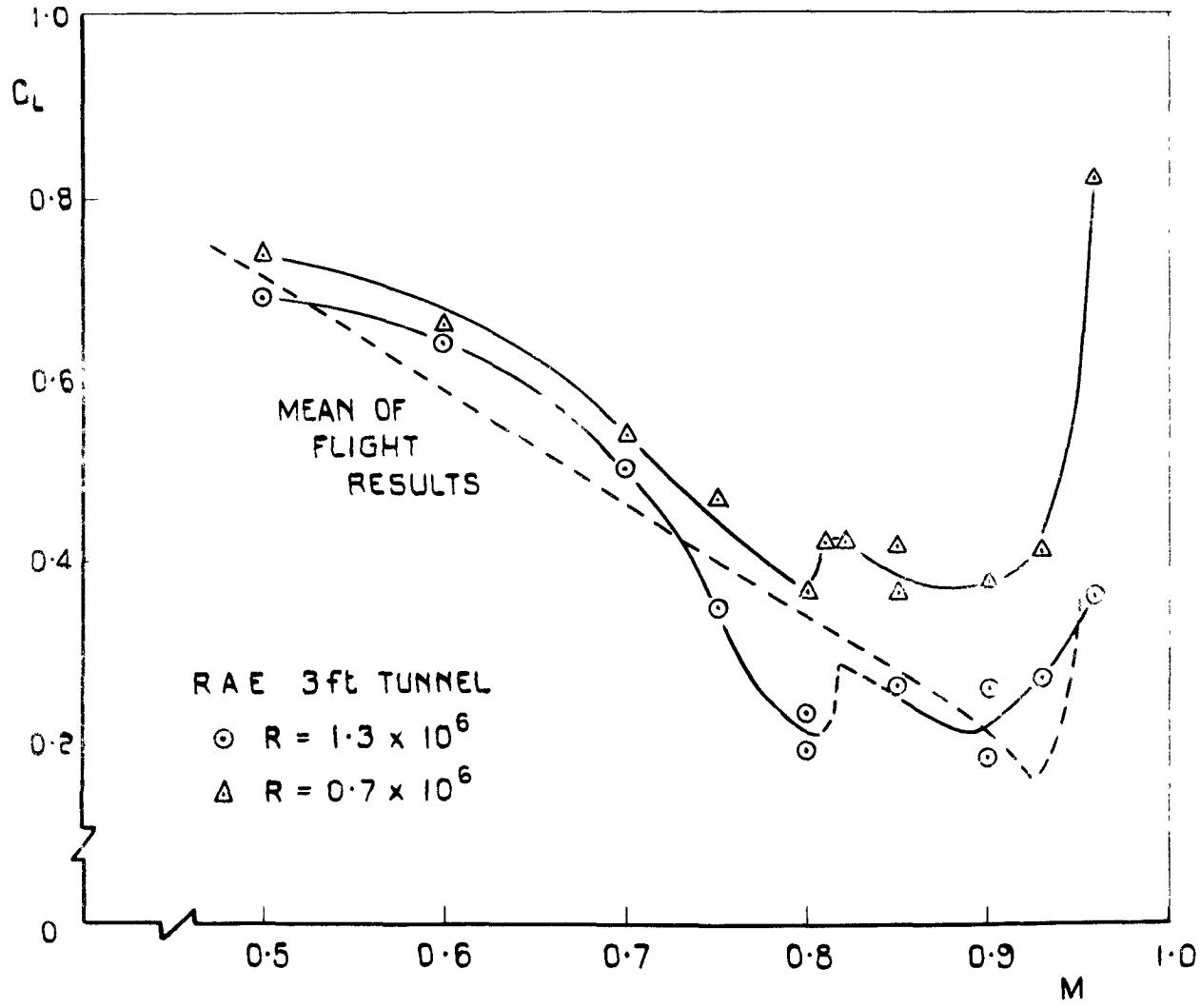

FIG. 6 MODEL A-COMPARISON OF TUNNEL BUFFET BOUNDARIES MEASURED AT TWO REYNOLDS NUMBERS

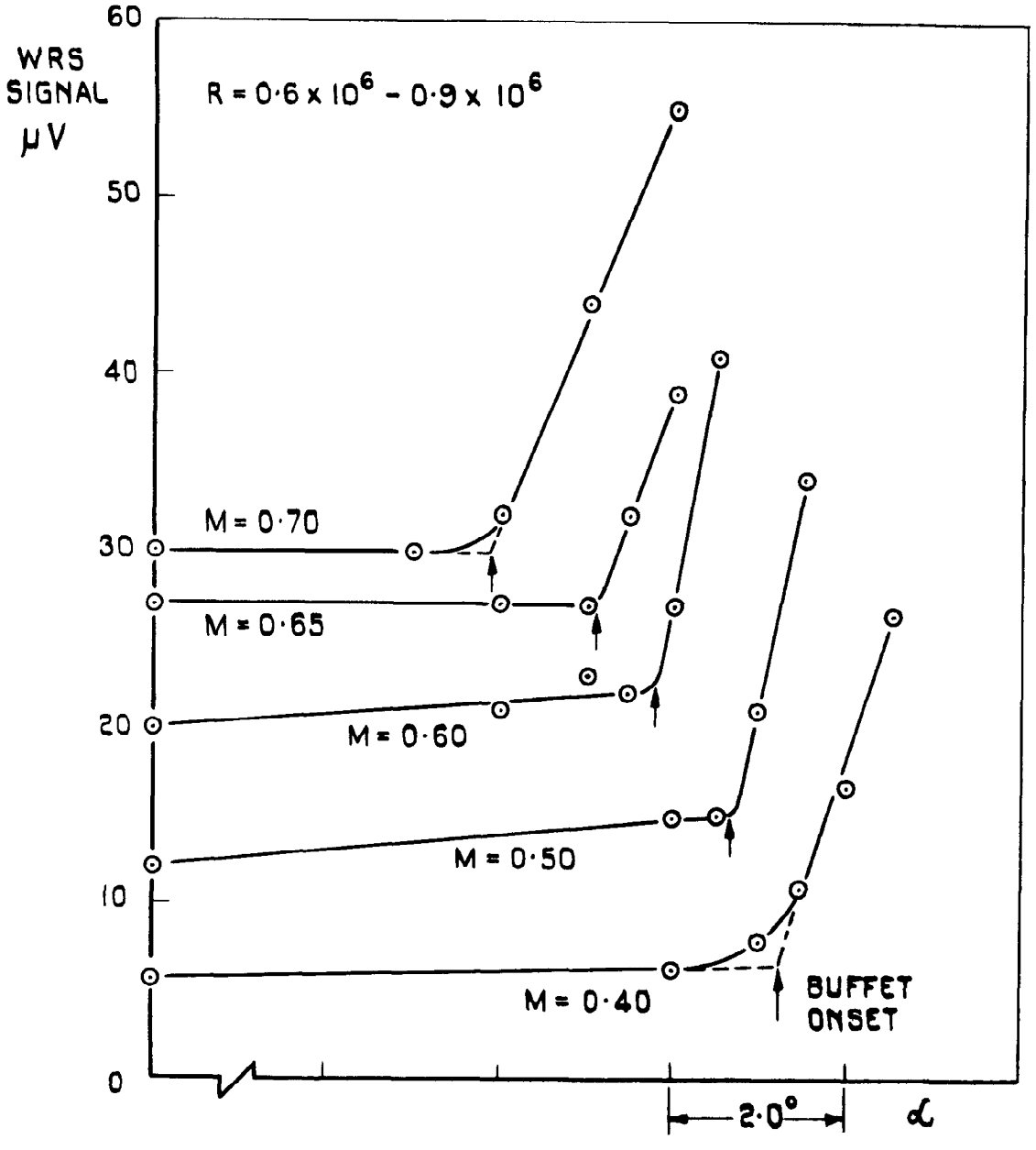

(a) M = 0.40 TO 0.70

FIG. 7 MODEL B - VARIATION OF WING - ROOT STRAIN SIGNAL WITH INCIDENCE - R A E 3FT TUNNEL

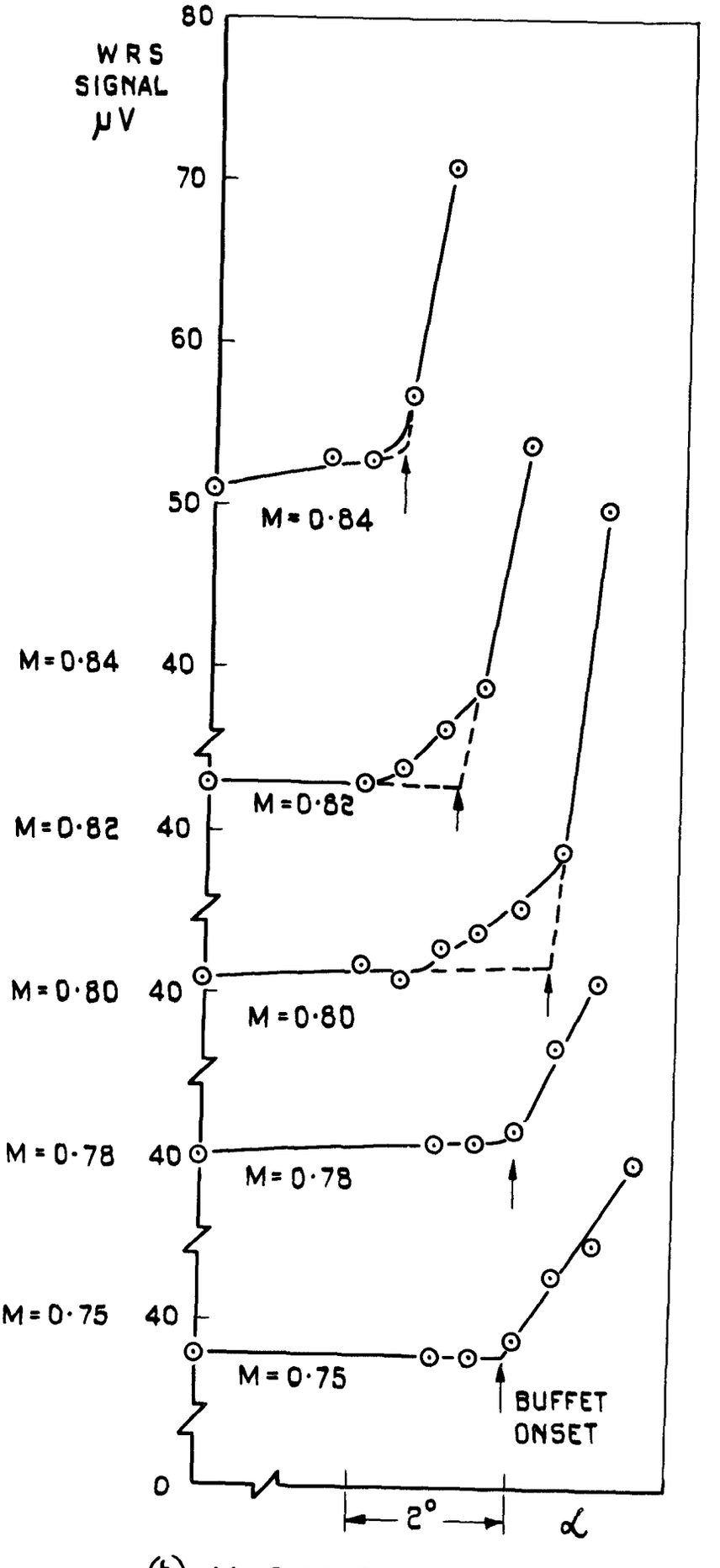

(b) M = 0.75 TO 0.84

FIG. 7 (CONTD)

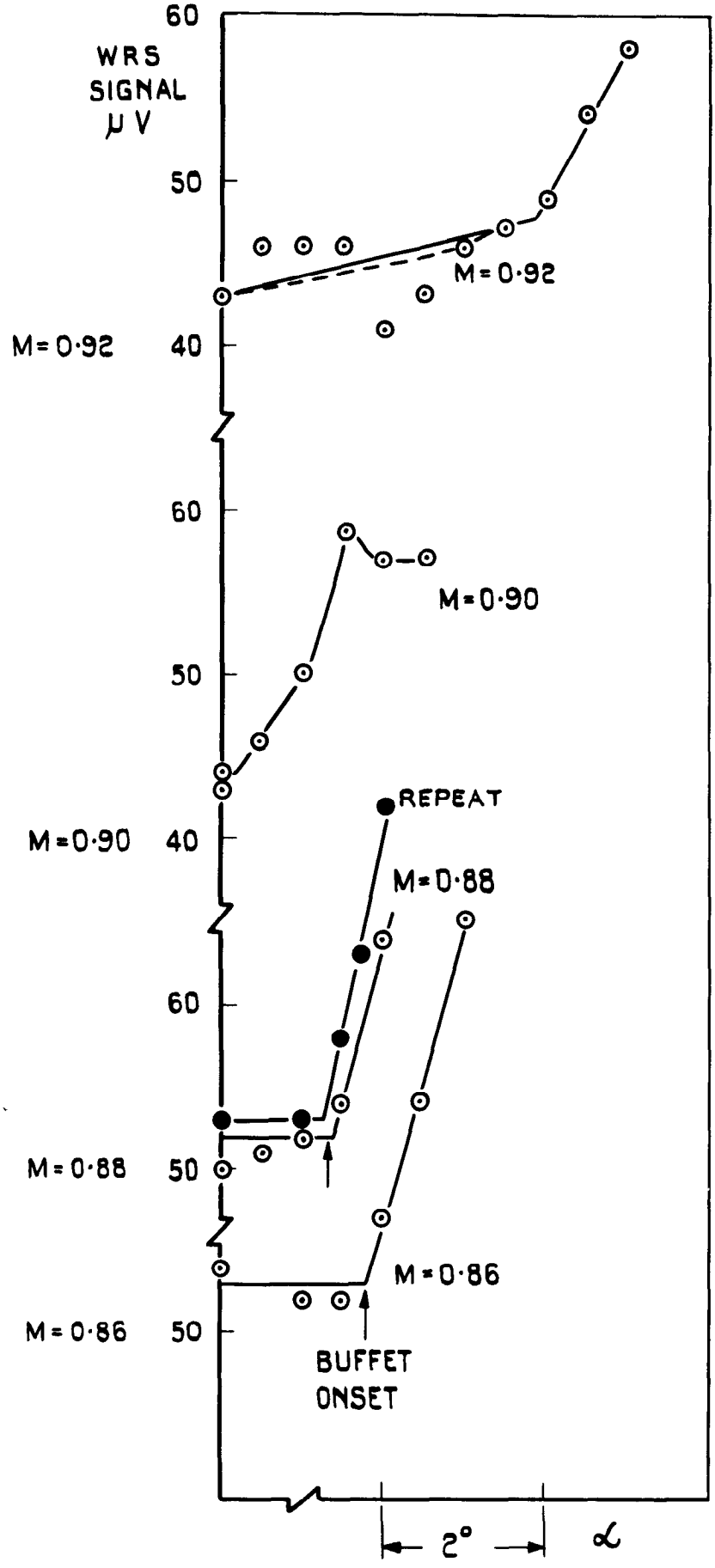

(c) M = 0·86 TO 0·92

FIG. 7 (CONCLD)

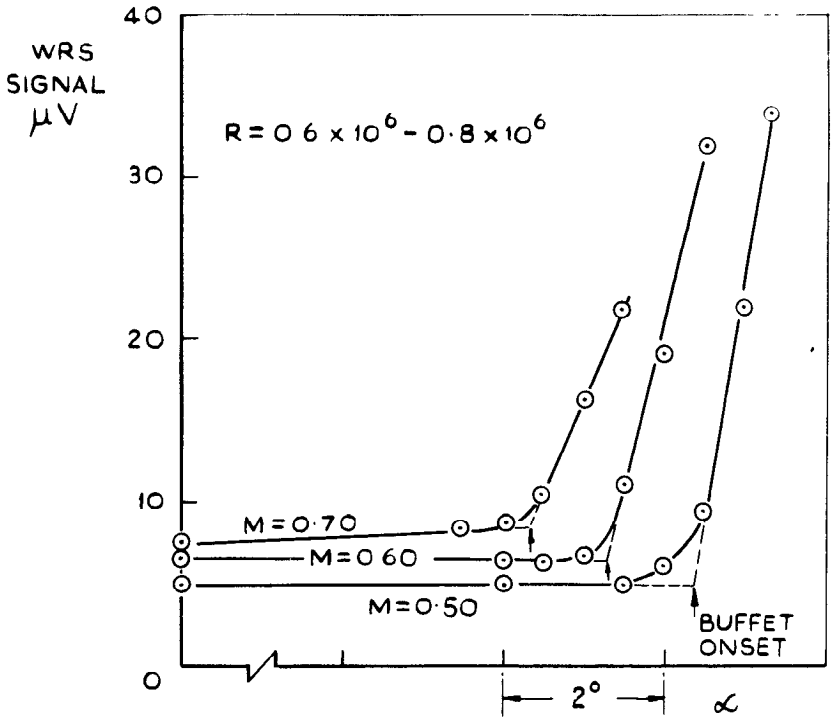

(a) M = 0·50 TO 0·70

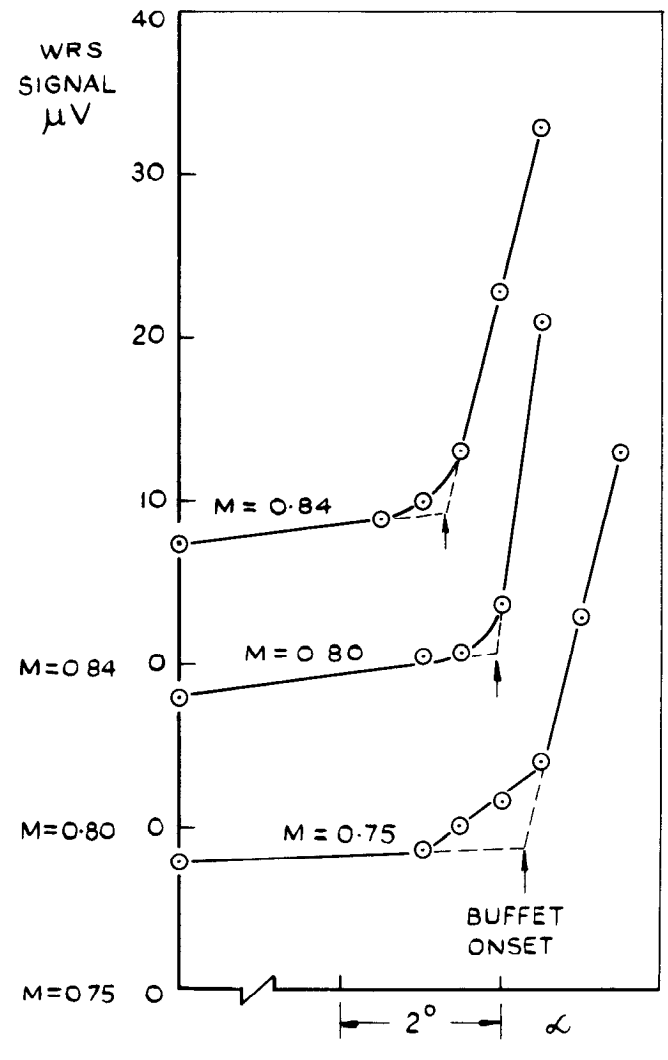

(b) M = 0·75 TO 0 84

FIG. 8 MODEL B - VARIATION OF WING-ROOT STRAIN SIGNAL WITH INCIDENCE - D H 2FT TUNNEL

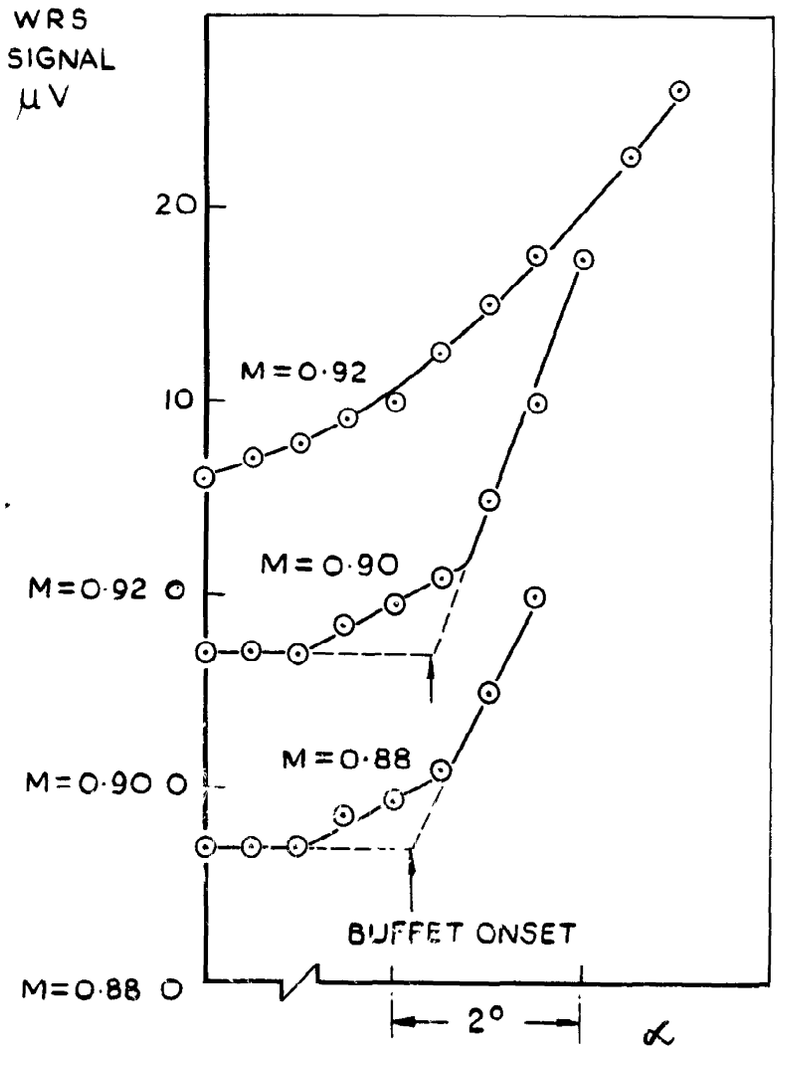

(c) M=0·88 TO 0·92

FIG. 8 (CONTD)

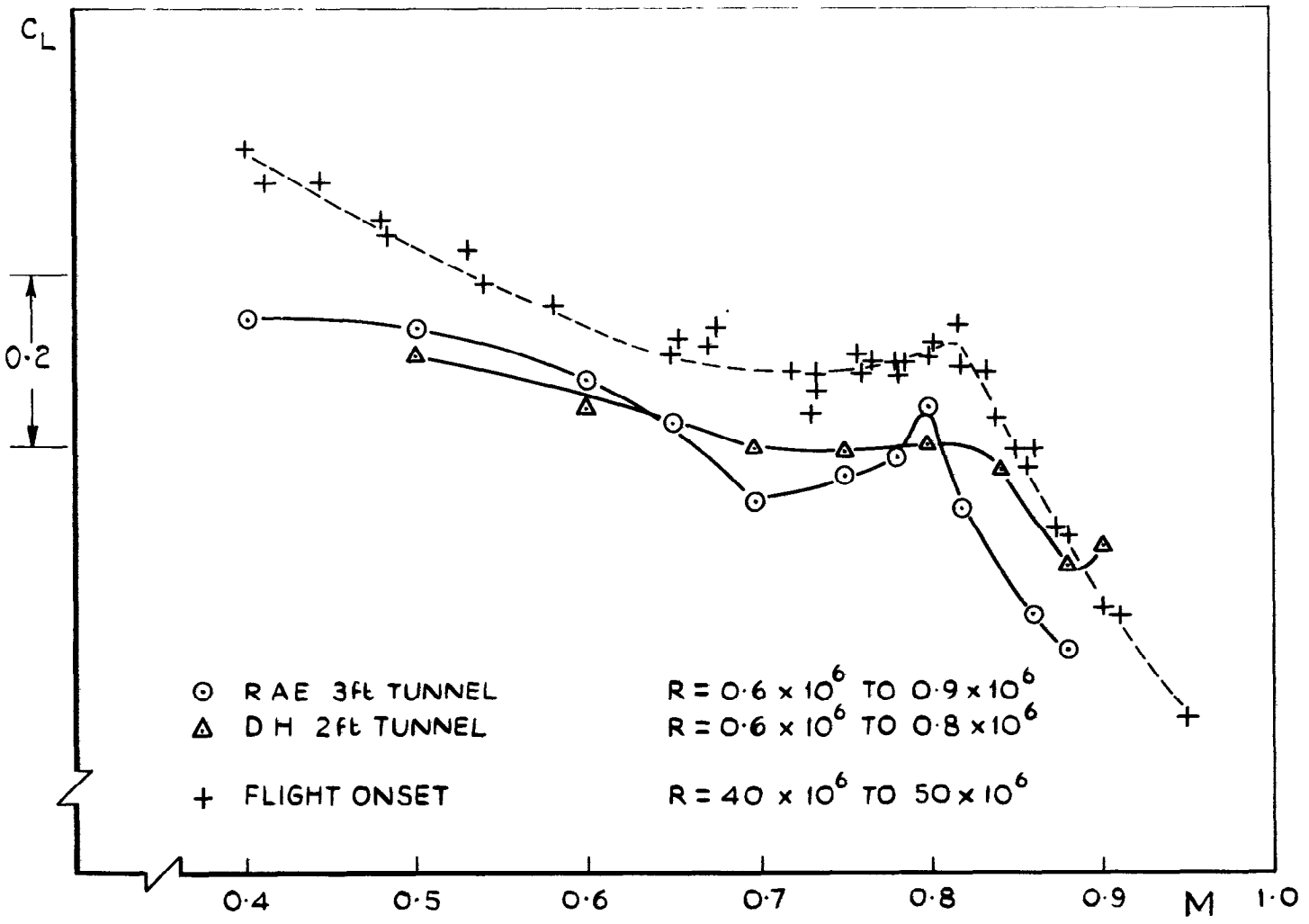

FIG.9 MODEL B – COMPARISON OF TUNNEL AND FLIGHT BUFFET BOUNDARIES

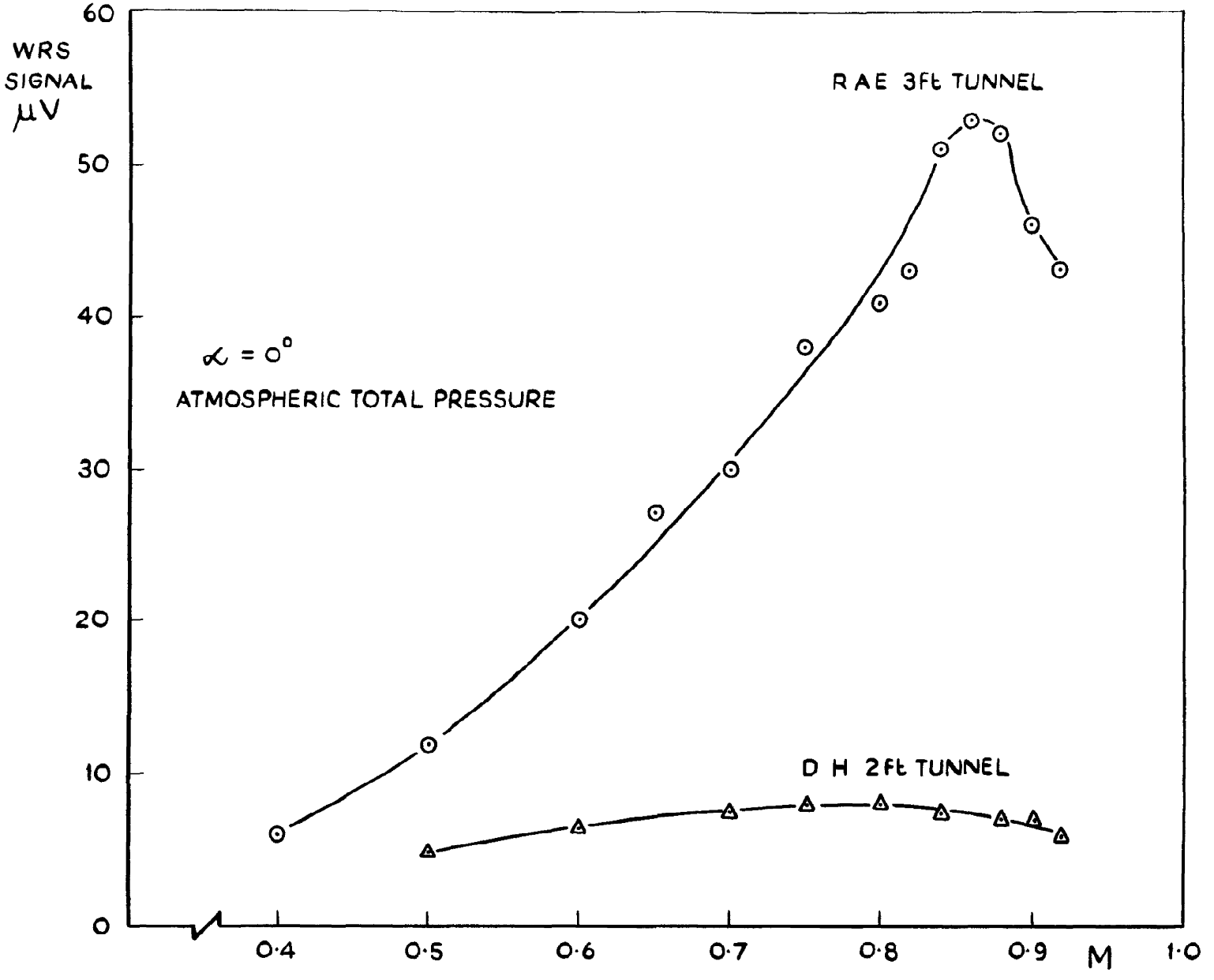

FIG. 10 MODEL B - WING RESPONSE TO FLOW UNSTEADINESS IN TWO TRANSONIC TUNNELS

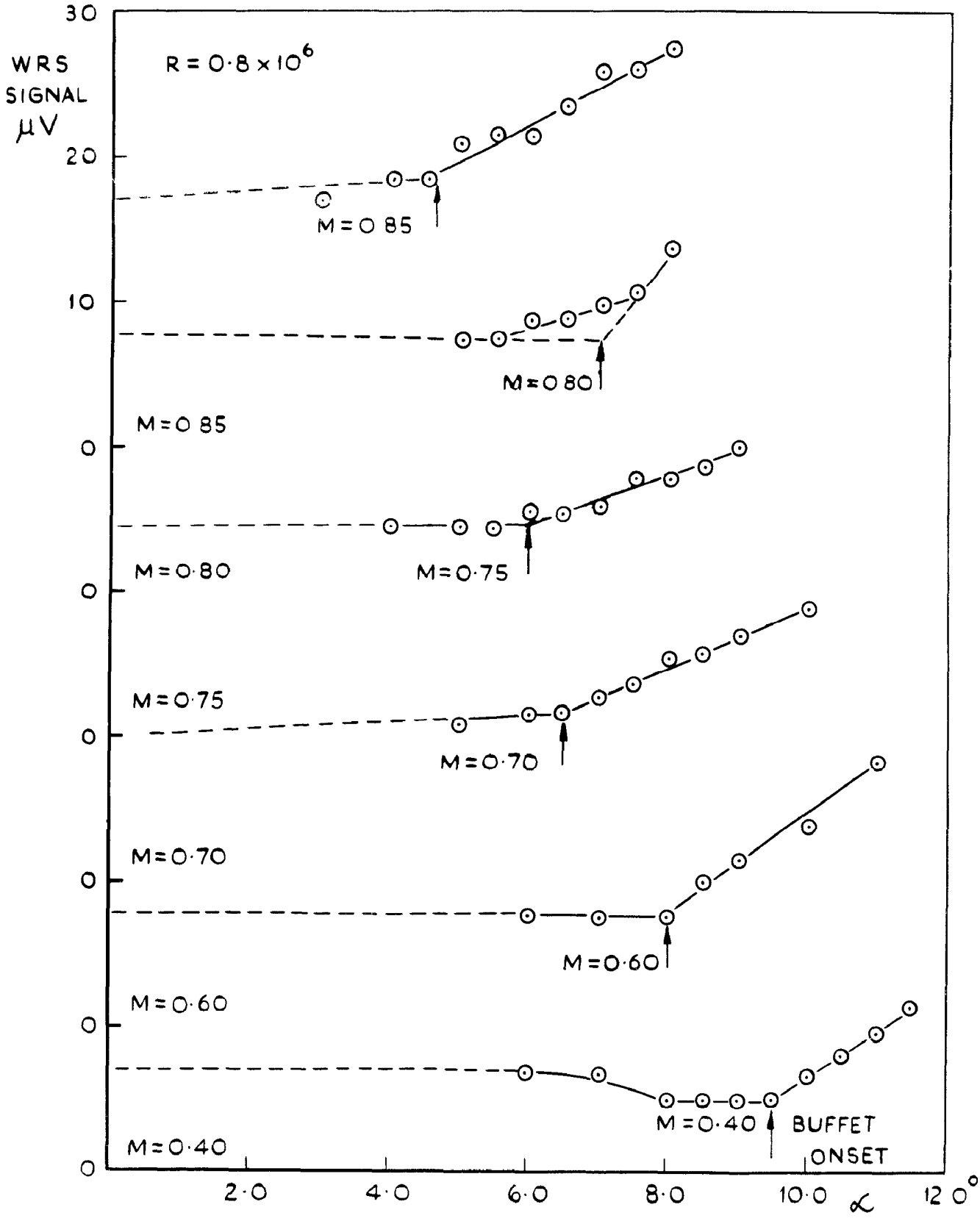

(a) M = 0·40 TO 0·85

FIG. 11 MODEL C - VARIATION OF WING - ROOT STRAIN SIGNAL WITH INCIDENCE - RAE 3FT TUNNEL

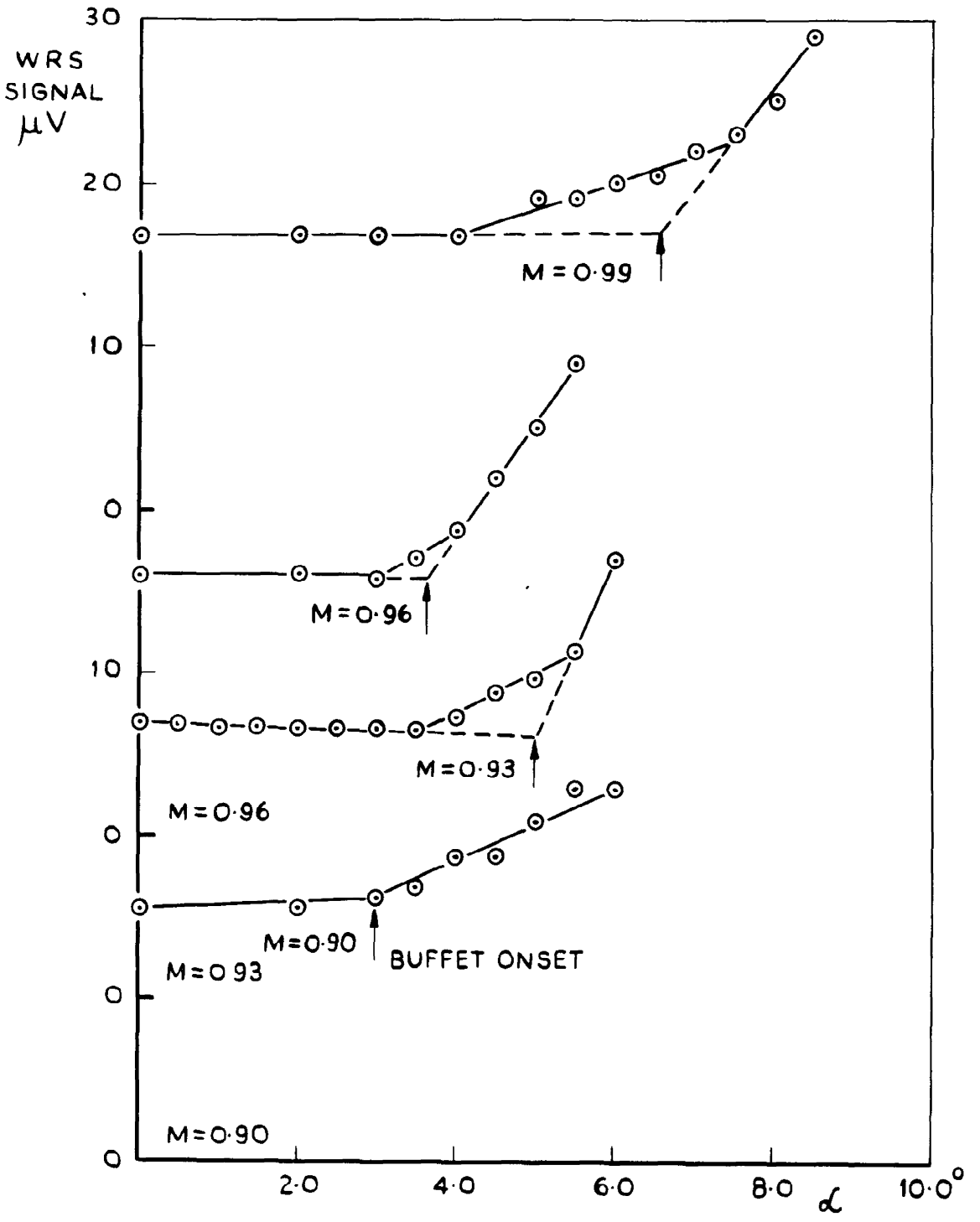

(b) M = 0·90 TO 0·99

FIG. 11 (CONTD)

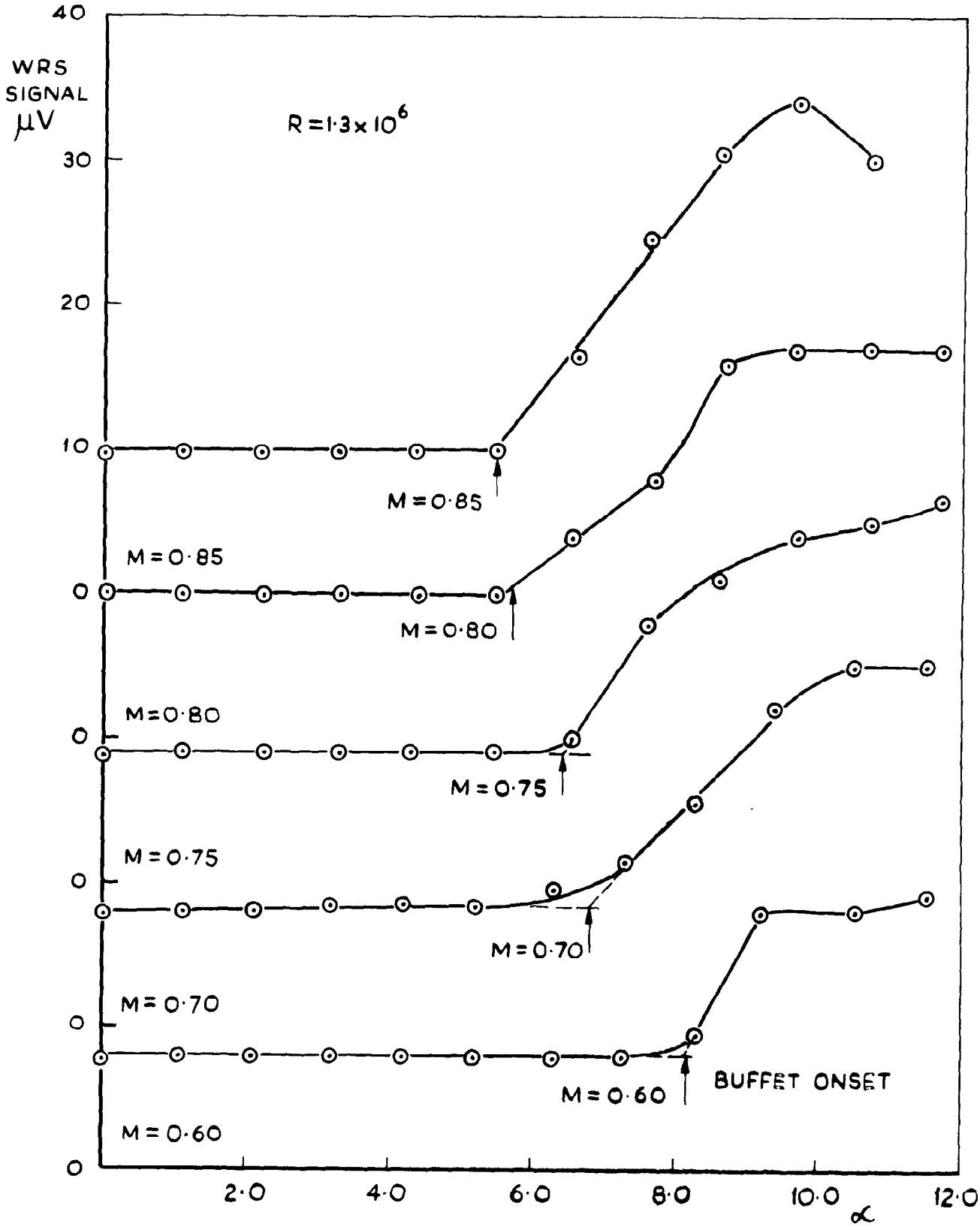

(a) M = 0·40 TO 0·85

FIG. 12 MODEL C - VARIATION OF WING-ROOT STRAIN SIGNAL WITH INCIDENCE ARA 8x9 FT TUNNEL

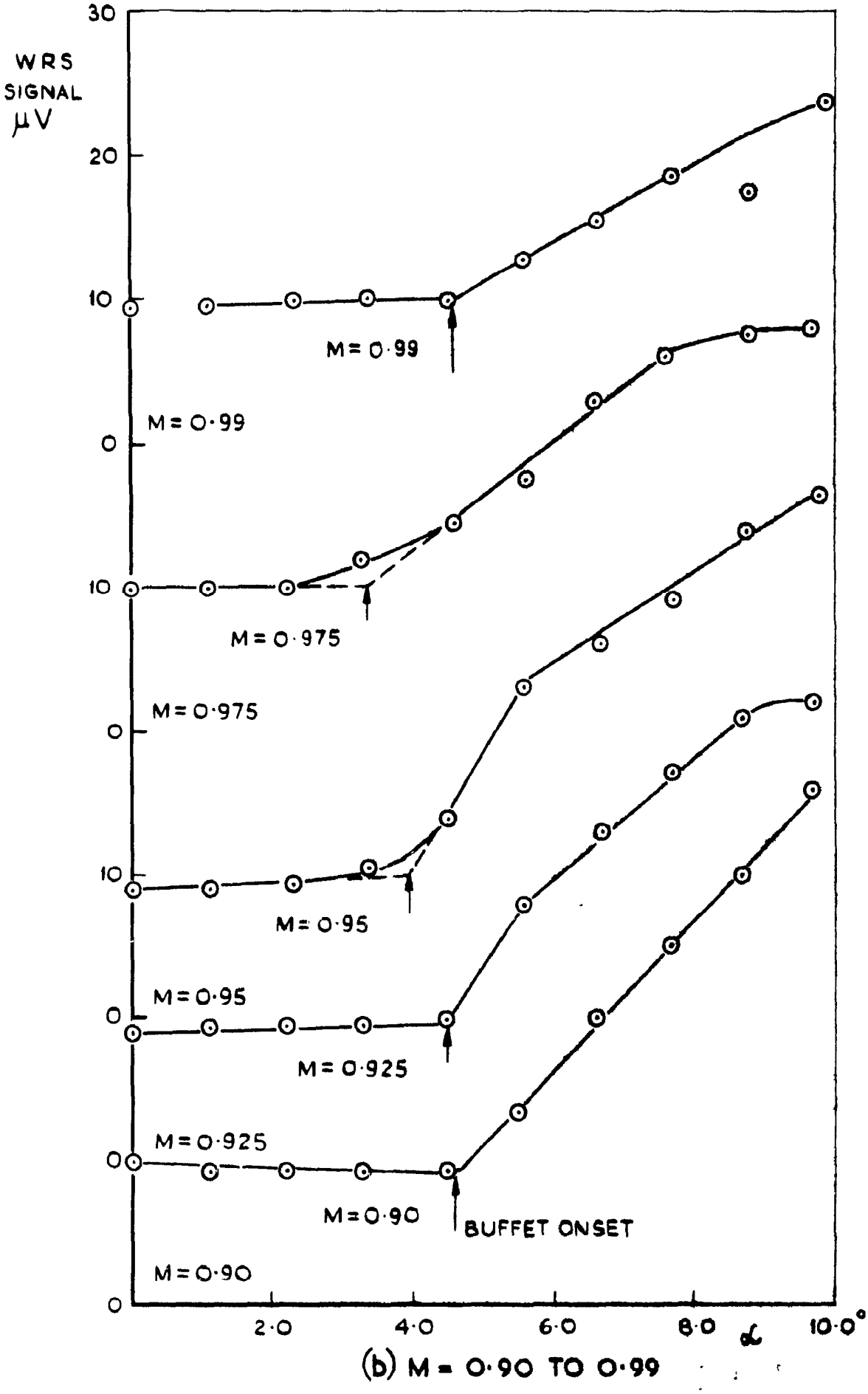

(b) M = 0·90 TO 0·99

FIG. 12 (CONTD)

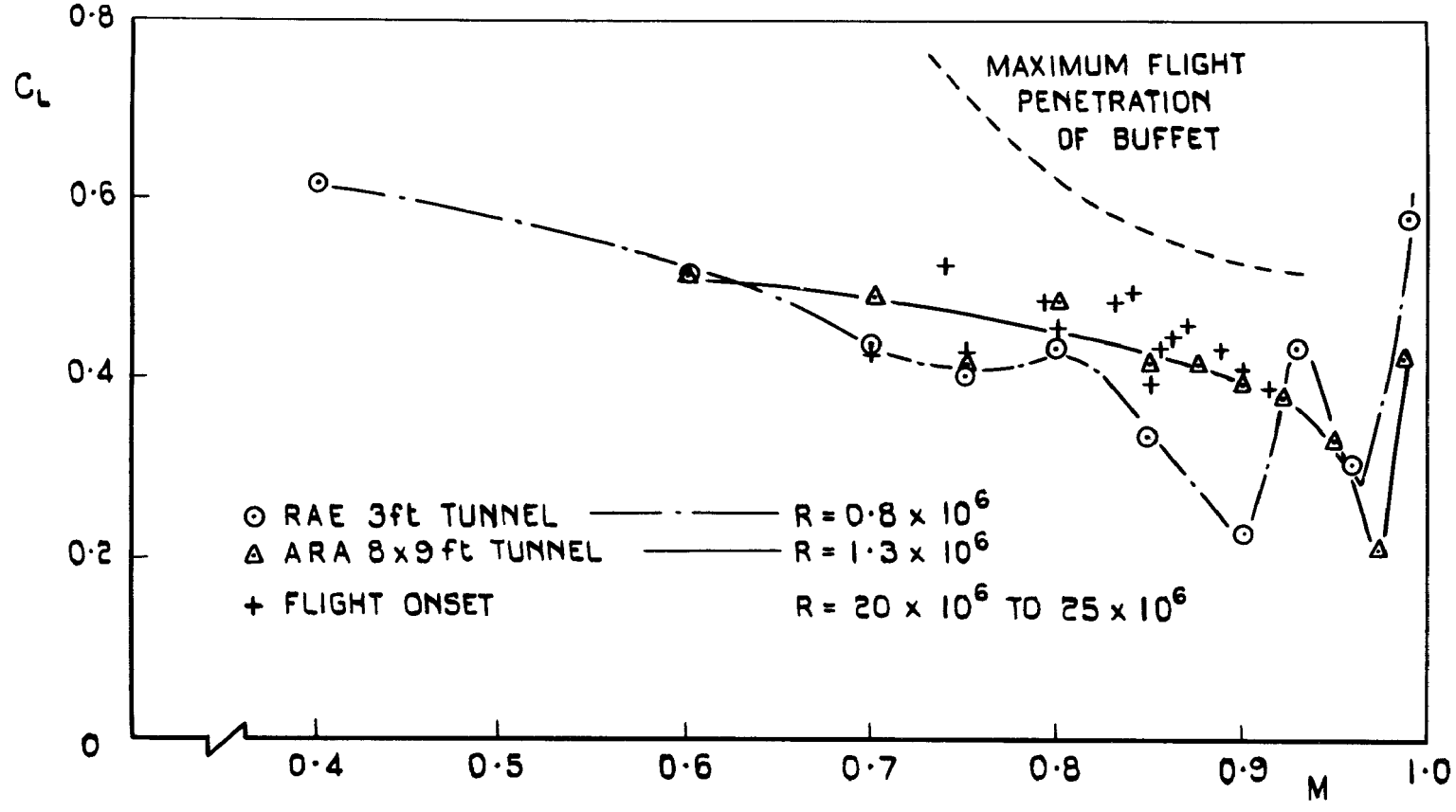

FIG. 13 MODEL C - COMPARISON OF TUNNEL AND FLIGHT BUFFET BOUNDARIES

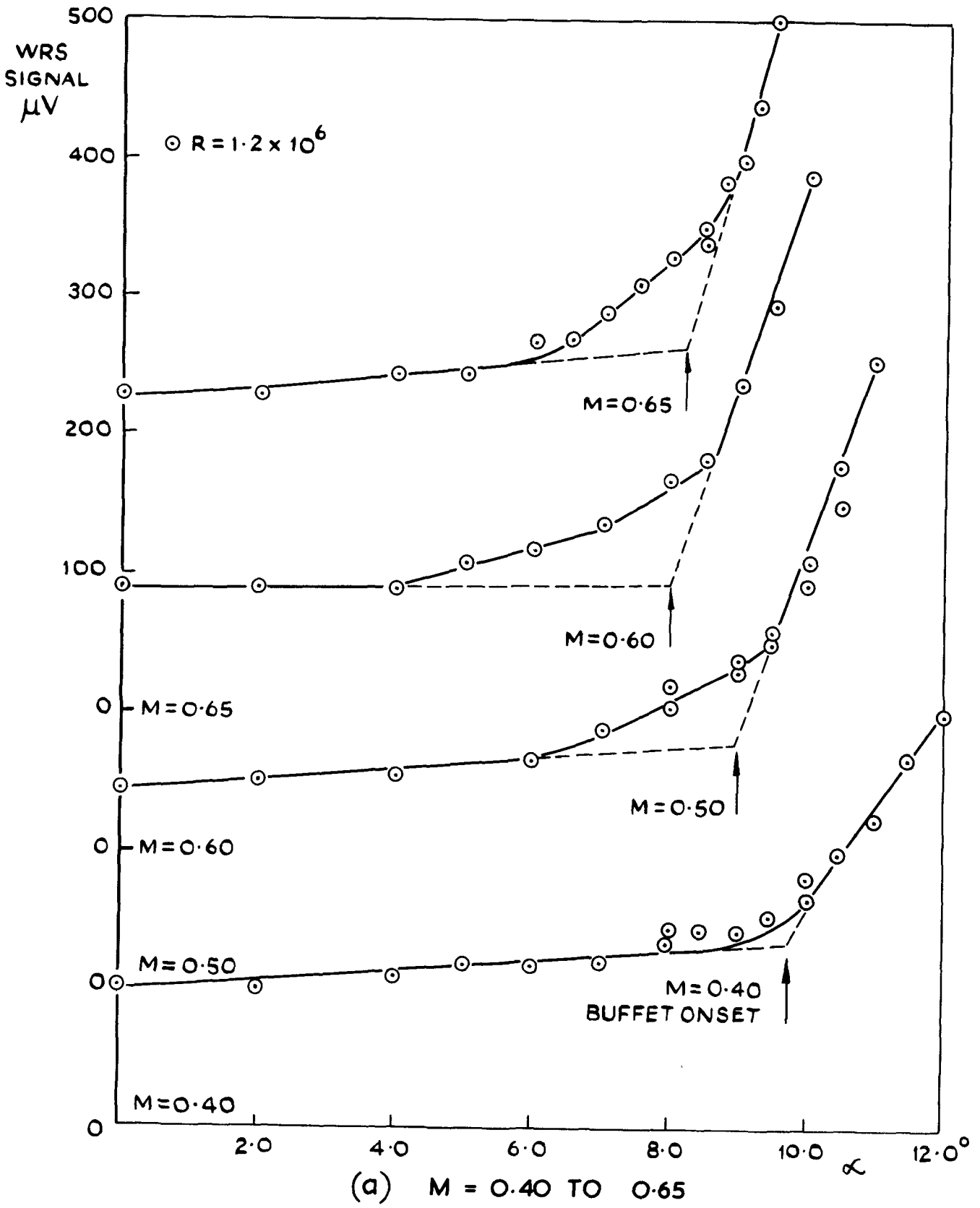

(a) M = 0.40 TO 0.65

FIG.14 MODEL D - VARIATION OF WING-ROOT STRAIN SIGNAL WITH INCIDENCE - RAE 3 FT TUNNEL

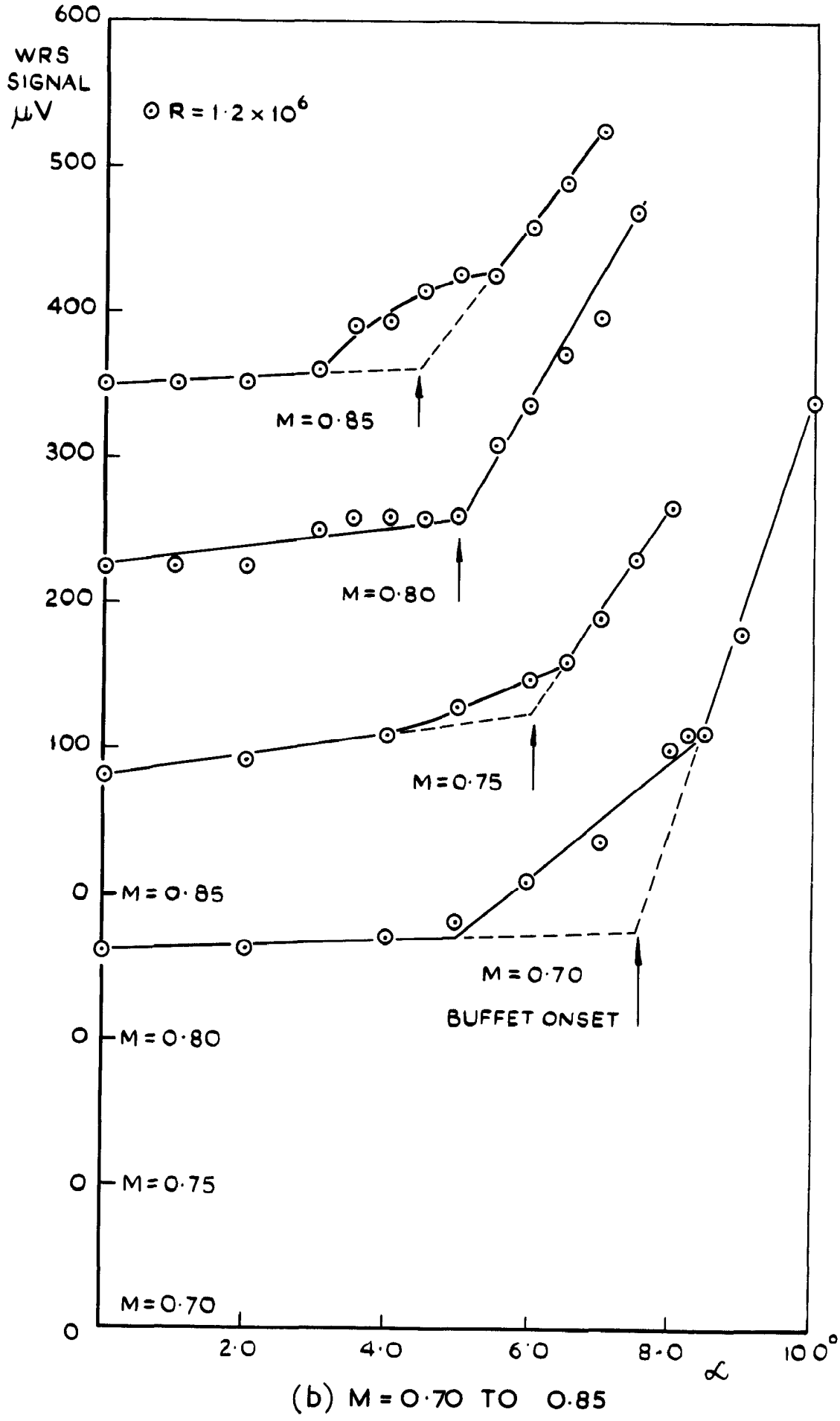

(b) M = 0·70 TO 0·85

FIG. 14 (CONTD)

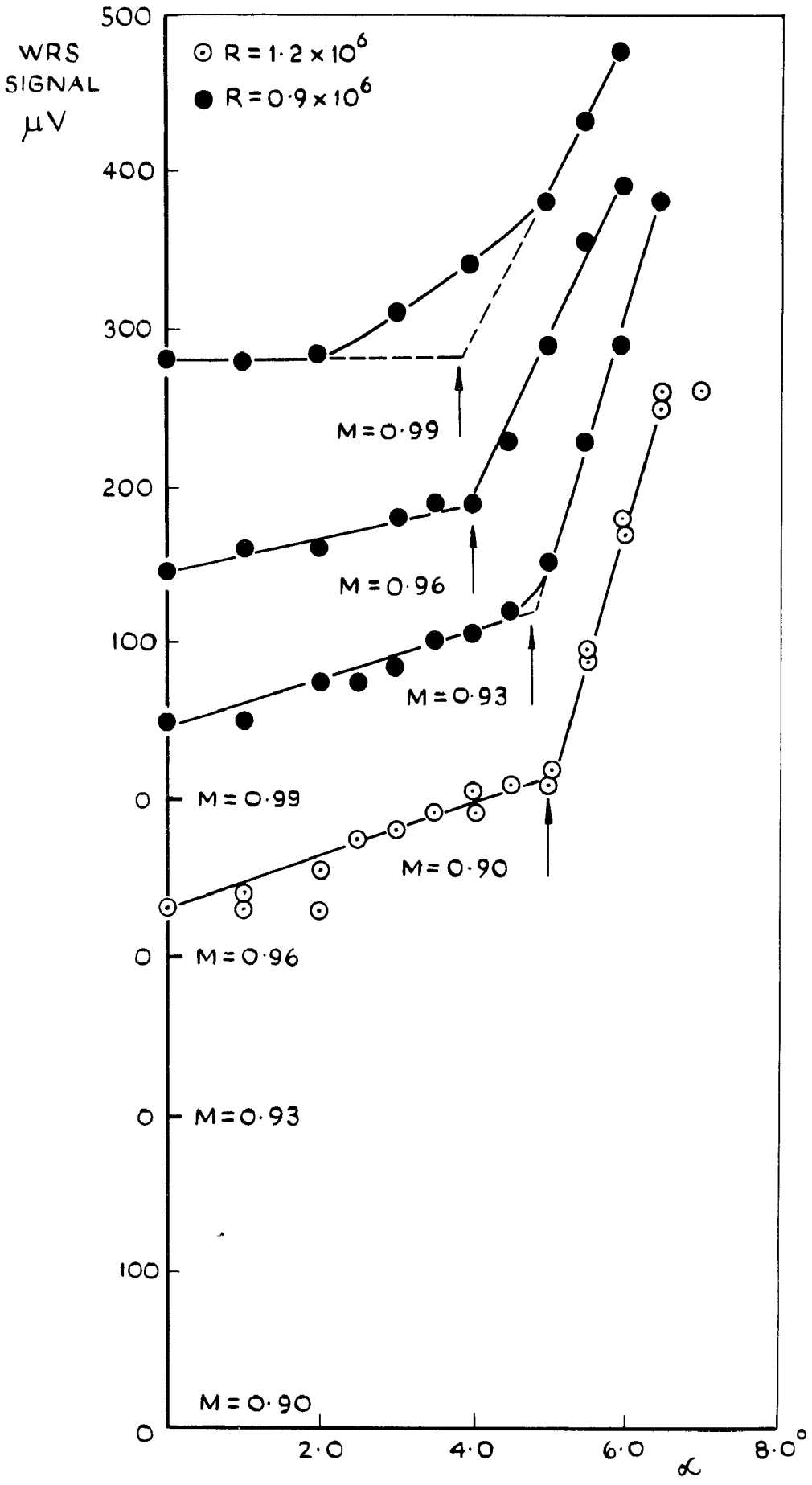

(c) M = 0·90 TO 0·99

FIG. 14 (CONCLD)

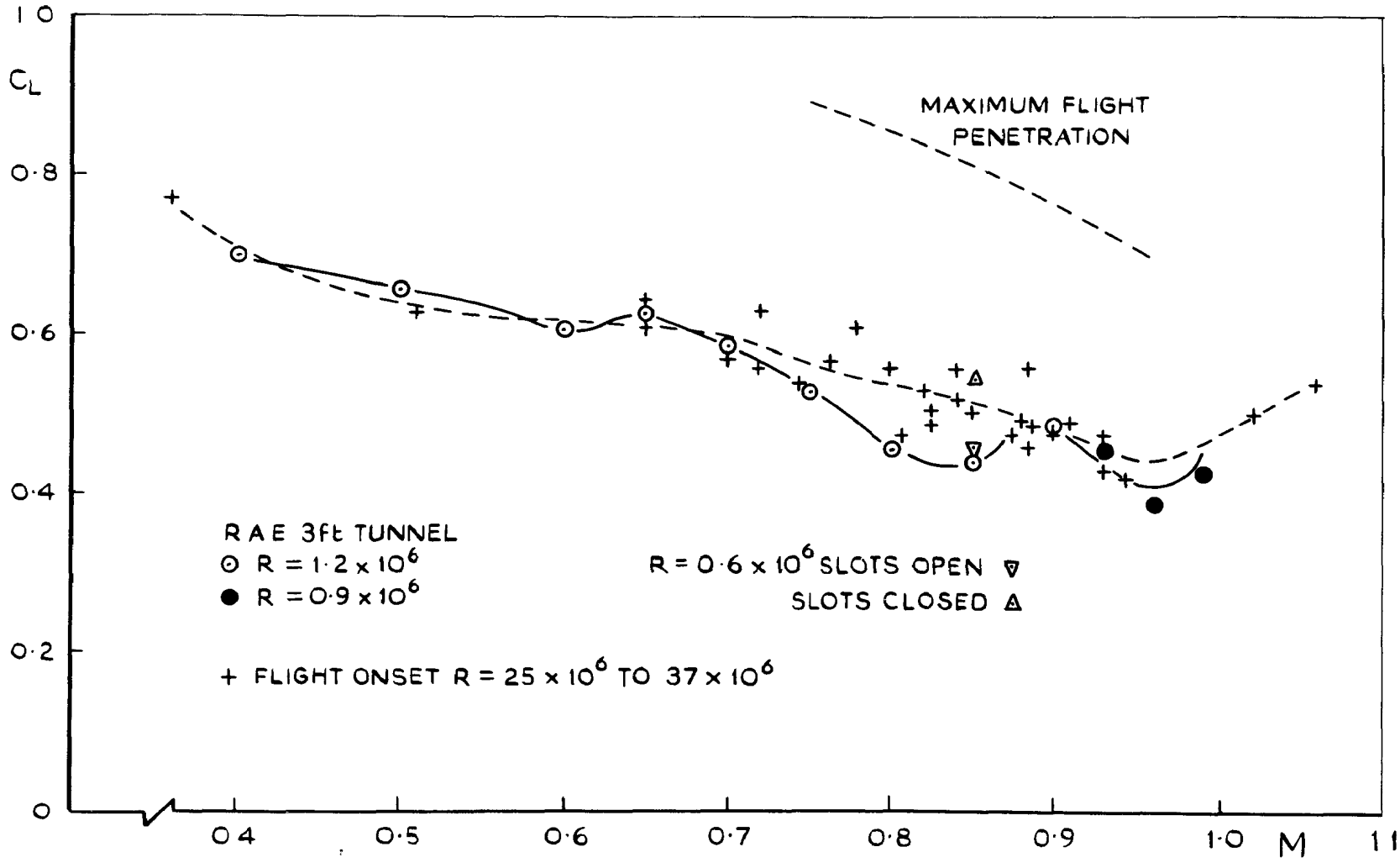

FIG. 15 MODEL D - COMPARISON OF TUNNEL AND FLIGHT BUFFET BOUNDARIES

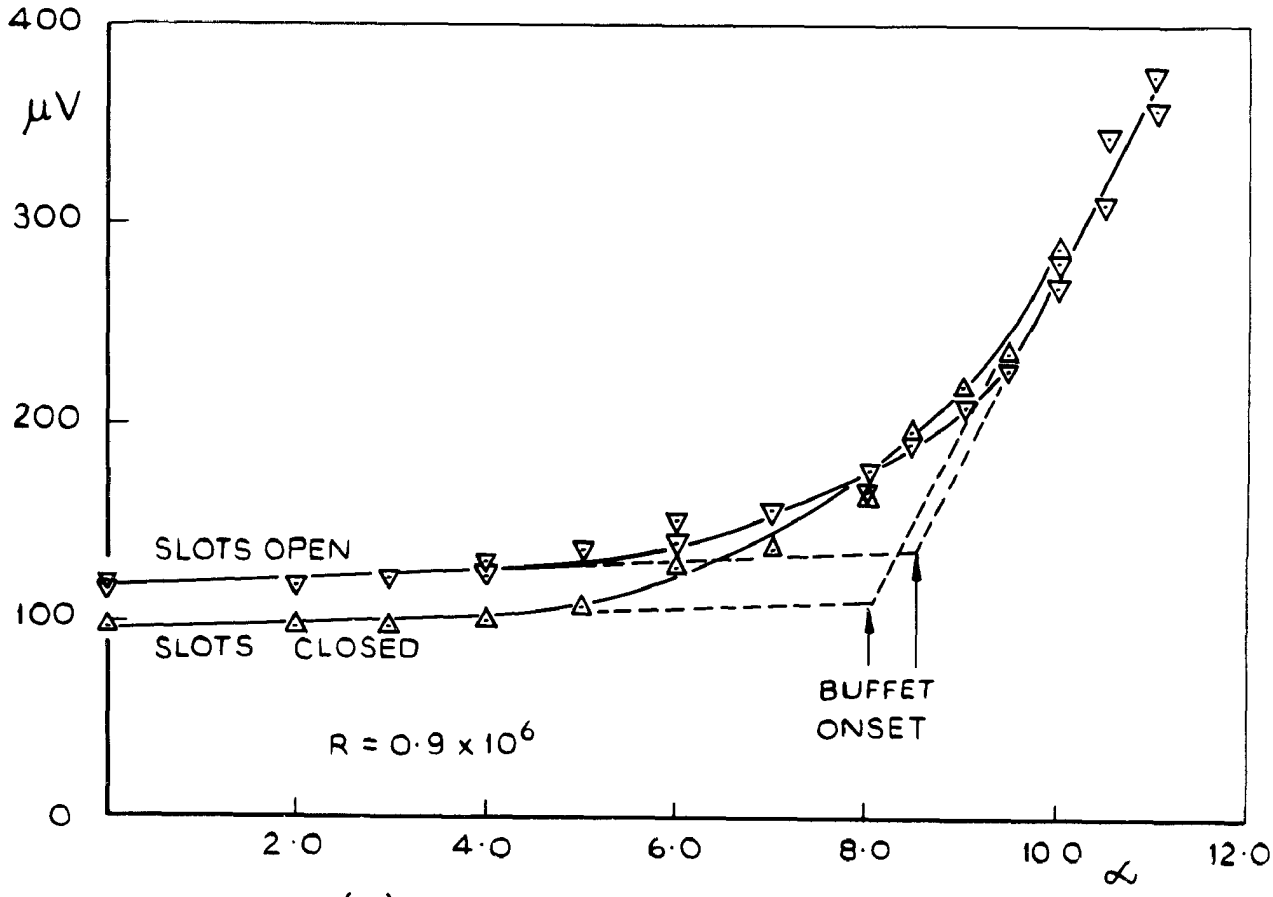

(a) M = 0 60

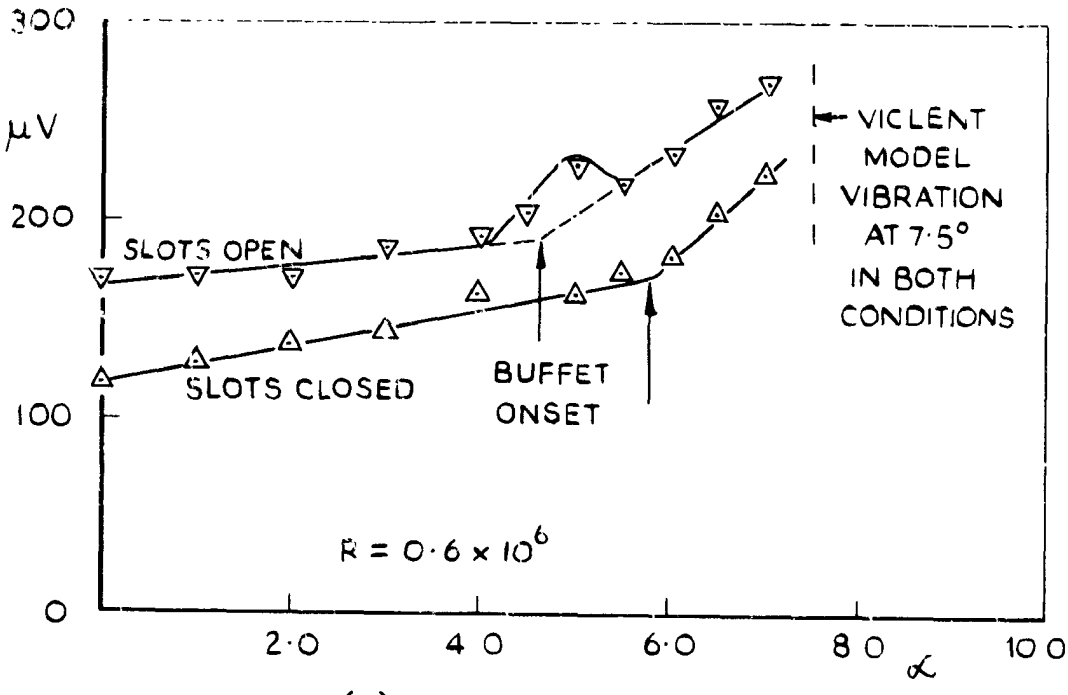

(b) M = 0·85

FIG. 16 MODEL D - VARIATION OF WING-ROOT STRAIN SIGNAL WITH INCIDENCE WITH SLOTS OPEN AND CLOSED

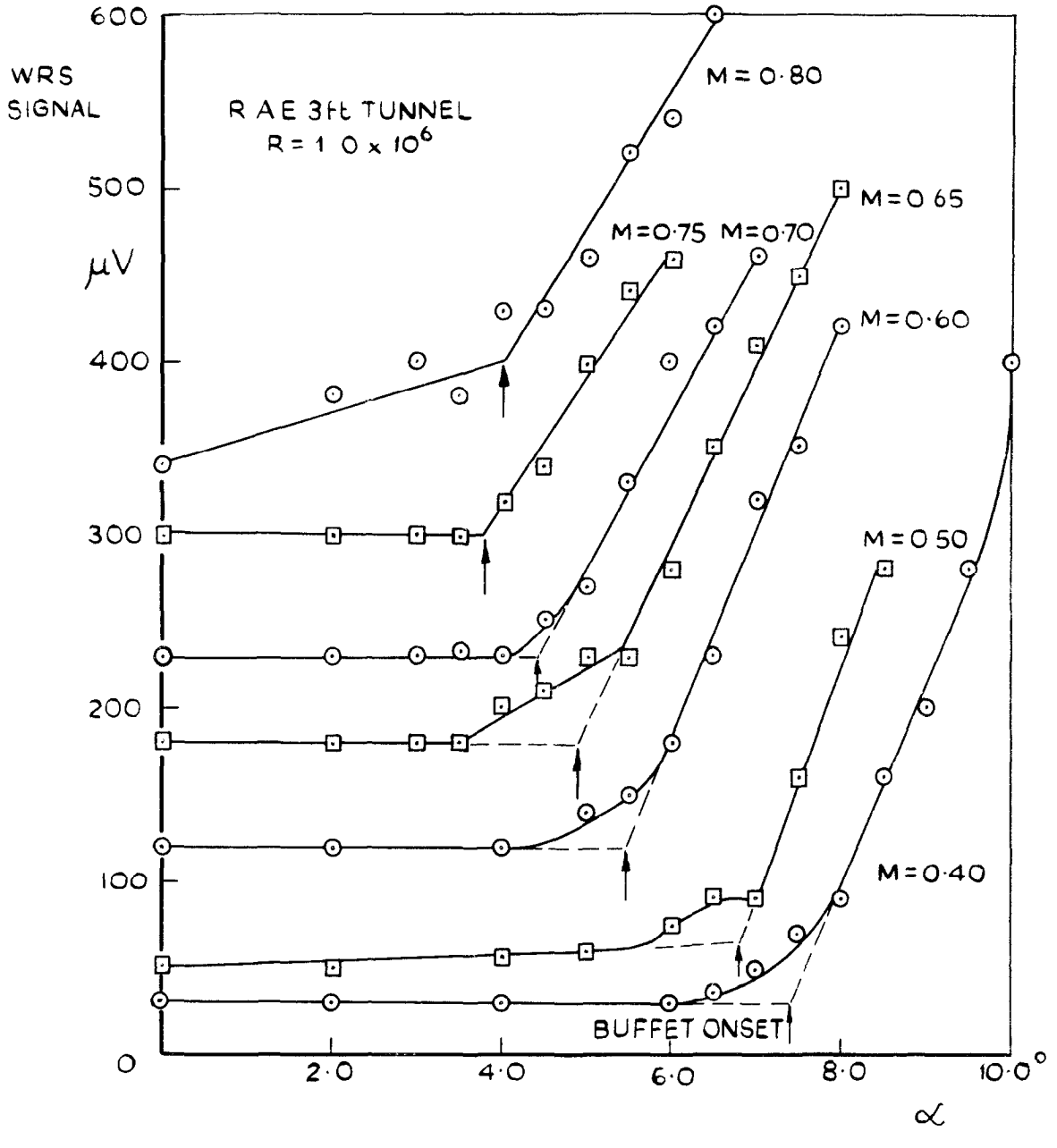

(a) M = 0·40 TO 0·80

FIG. 17 MODEL E - VARIATION OF WING-ROOT STRAIN SIGNAL WITH INCIDENCE

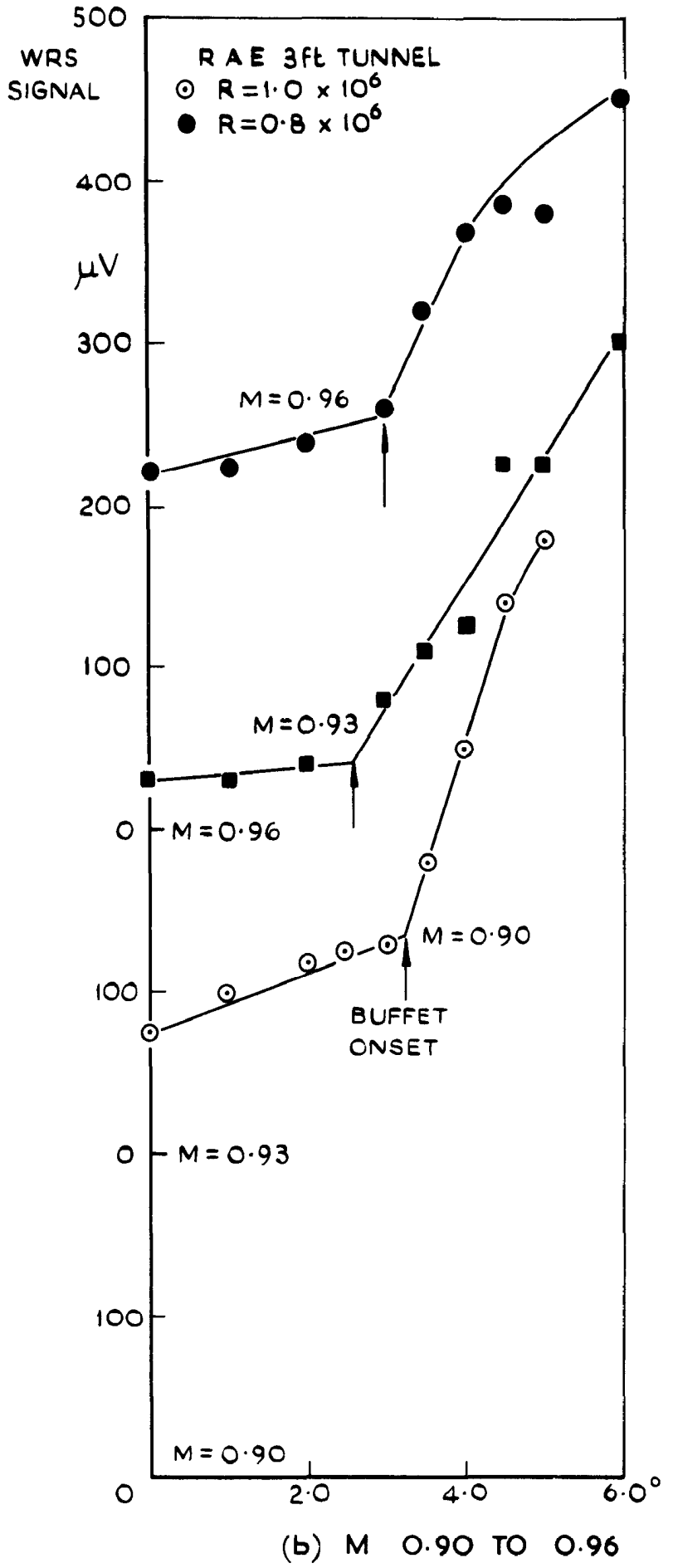

(b) M 0·90 TO 0·96

FIG. 17 (CONCLD)

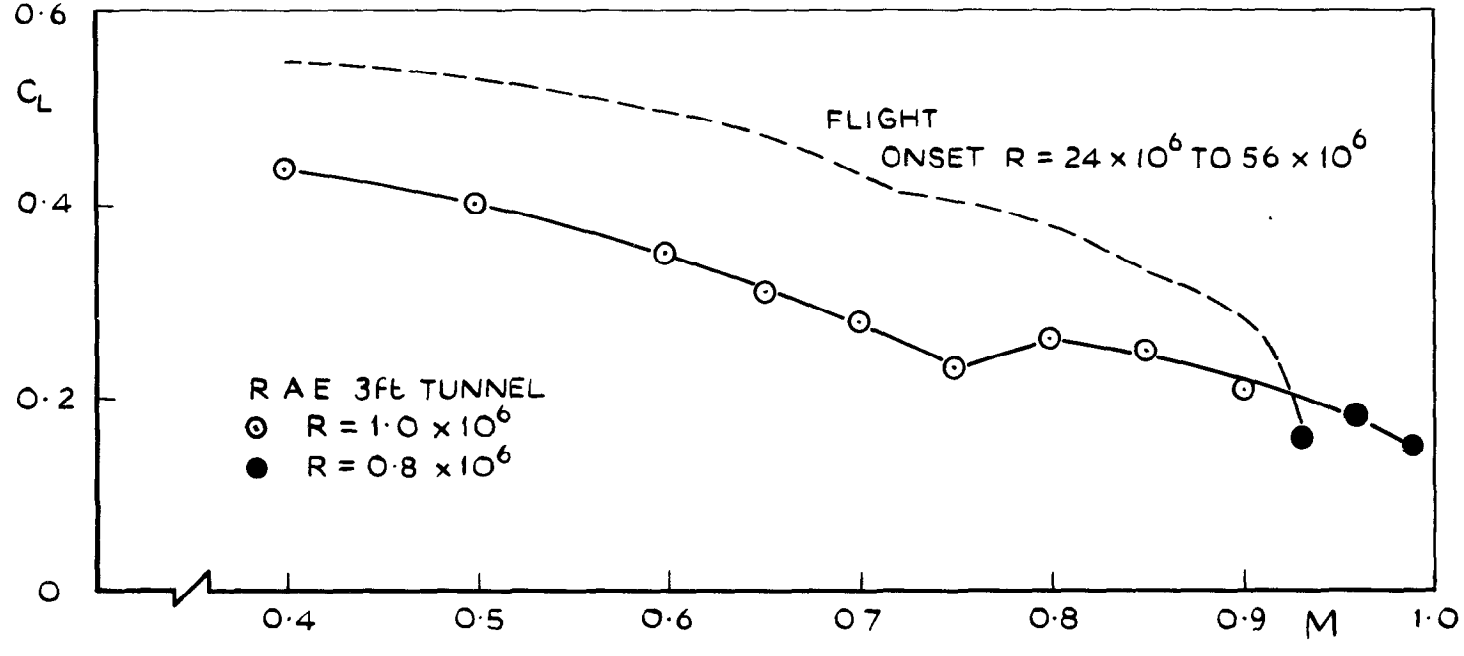

FIG. 18 MODEL E - COMPARISON OF TUNNEL AND FLIGHT BUFFET BOUNDARIES

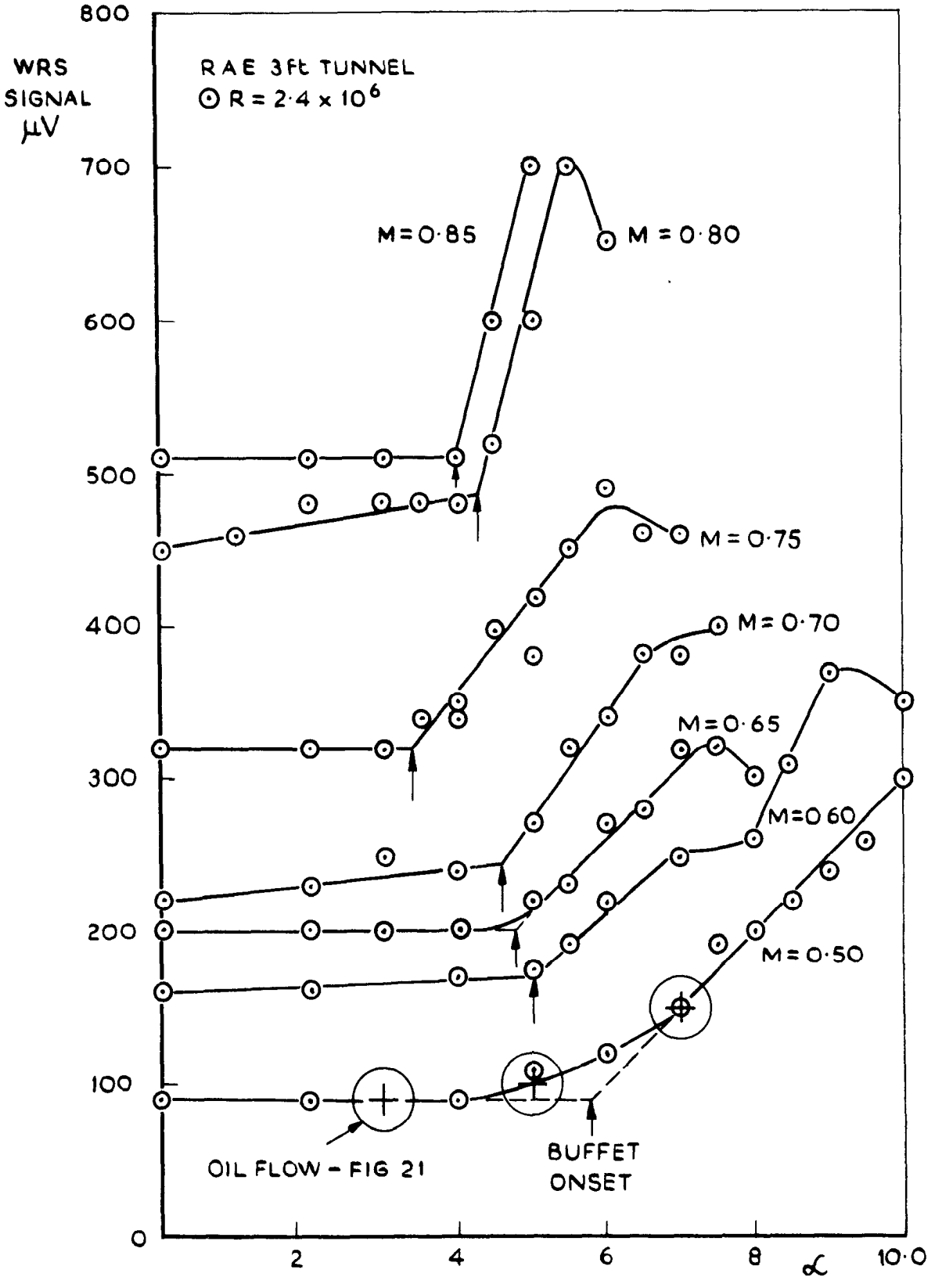

(a) M = 0·50 TO 0·85.

FIG. 19 MODEL F- VARIATION OF WING – ROOT STRAIN SIGNAL WITH INCIDENCE

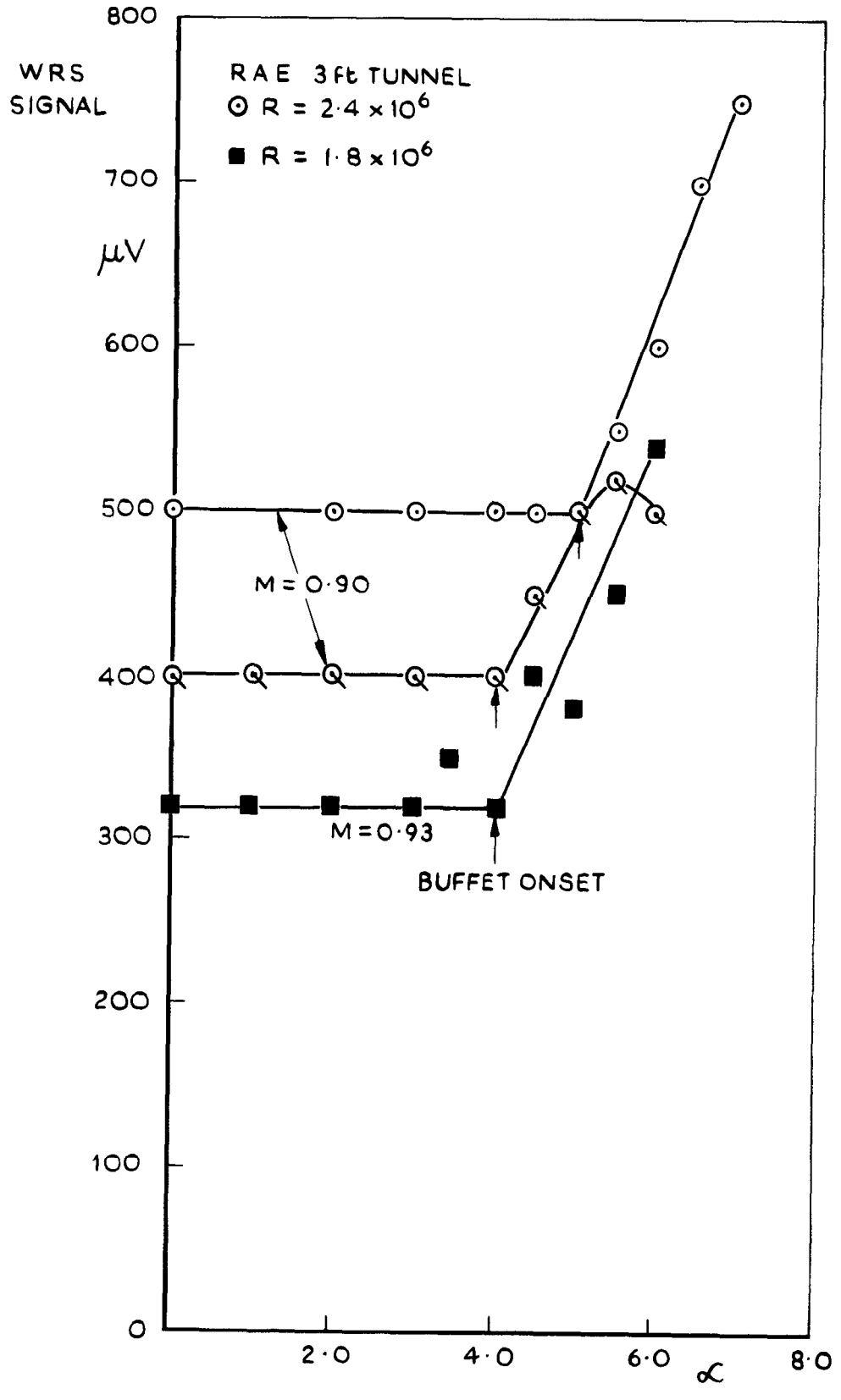

(b) M = 0·90 AND 0·93

FIG. 19 (CONCLD)

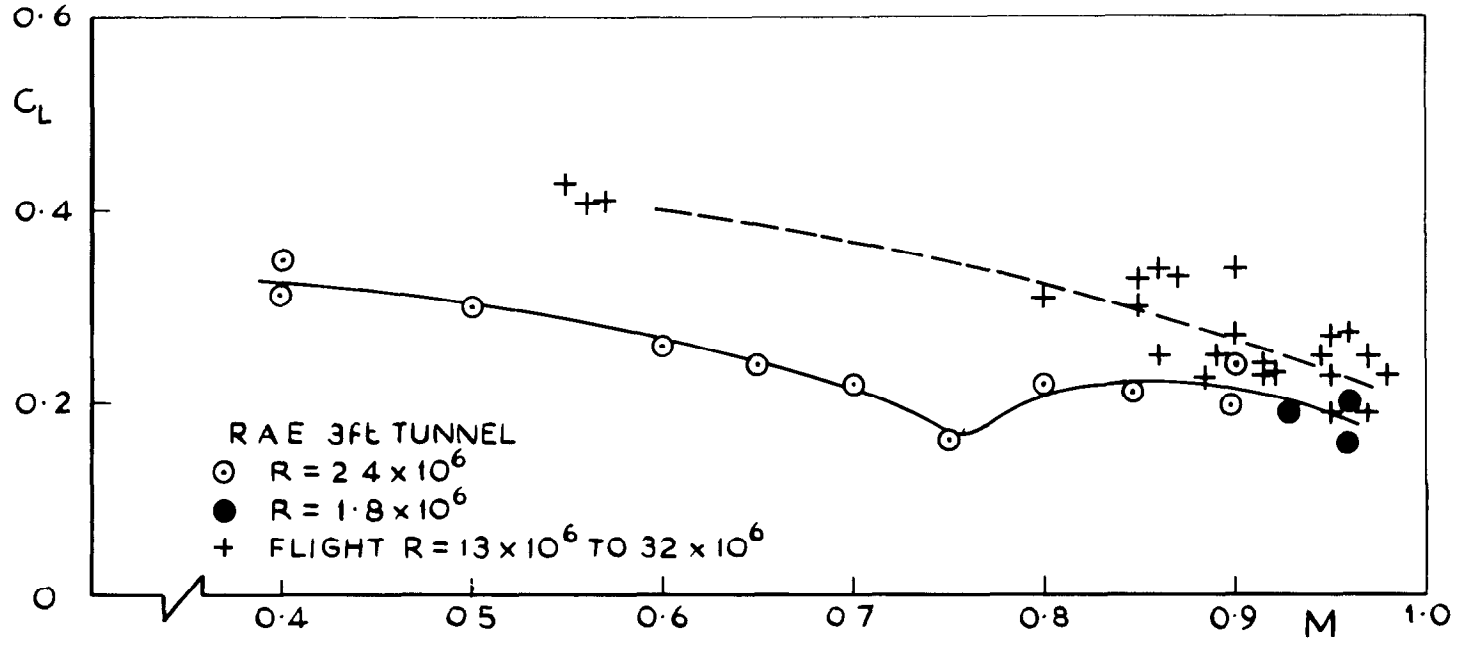

FIG. 20 MODEL F - COMPARISON OF TUNNEL AND FLIGHT BUFFET BOUNDARIES

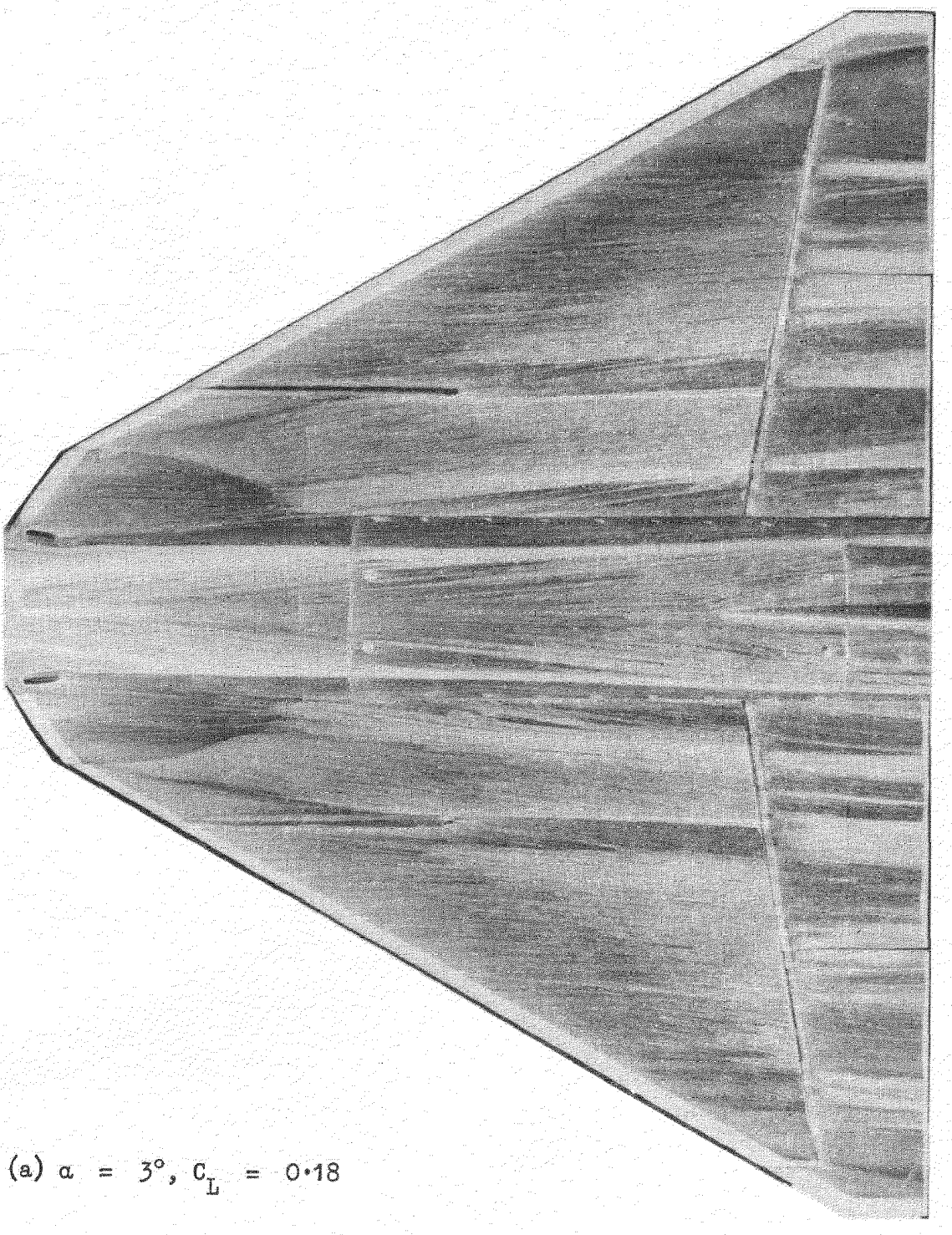

(a) $\alpha = 3°$, $C_L = 0{\cdot}18$

Fig. 21. Model F-oil flow photographs near buffet onset. M=0·50

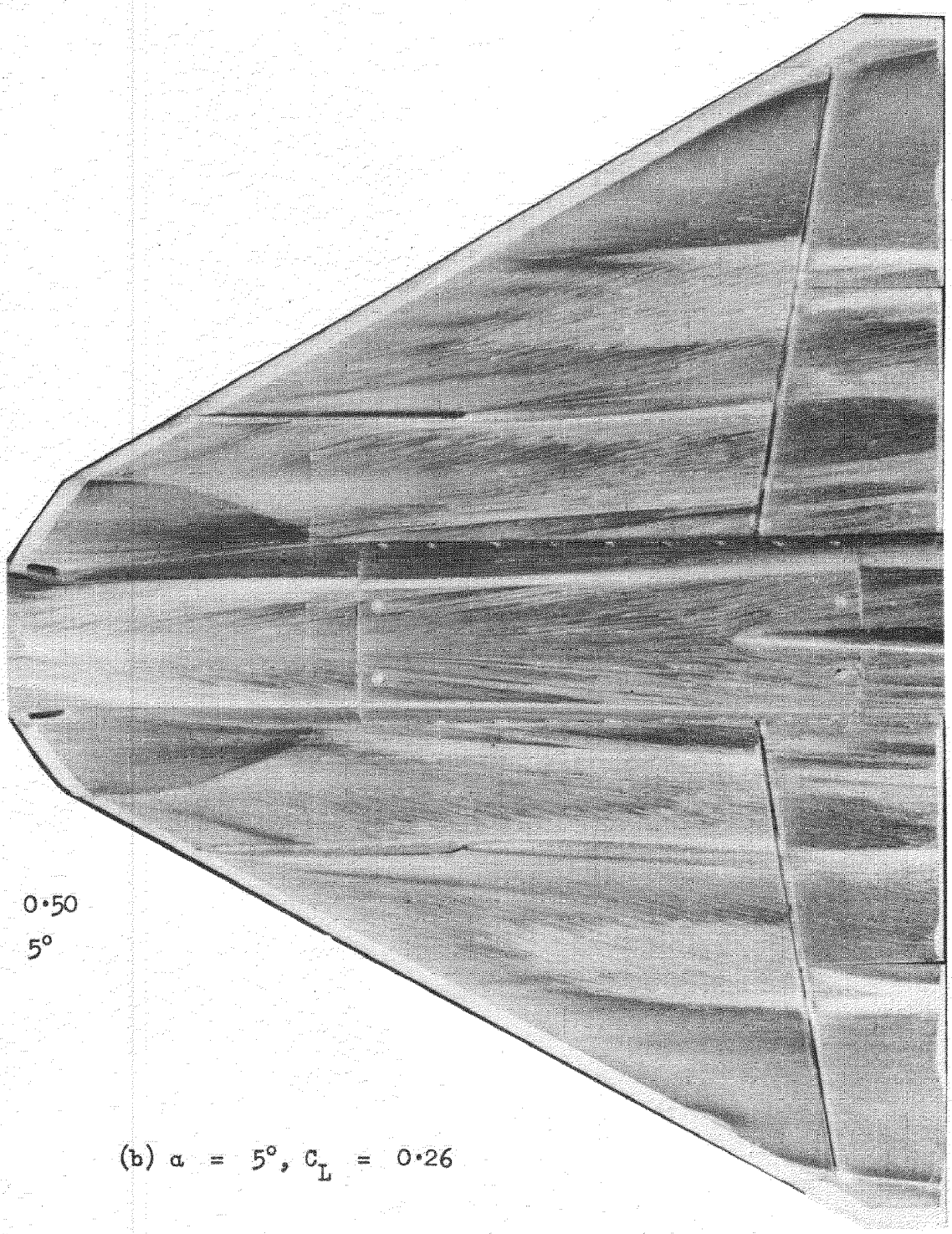

M = 0·50

α = 5°

(b) $\alpha = 5°$, $C_L = 0{\cdot}26$

Fig. 21 Cont'd

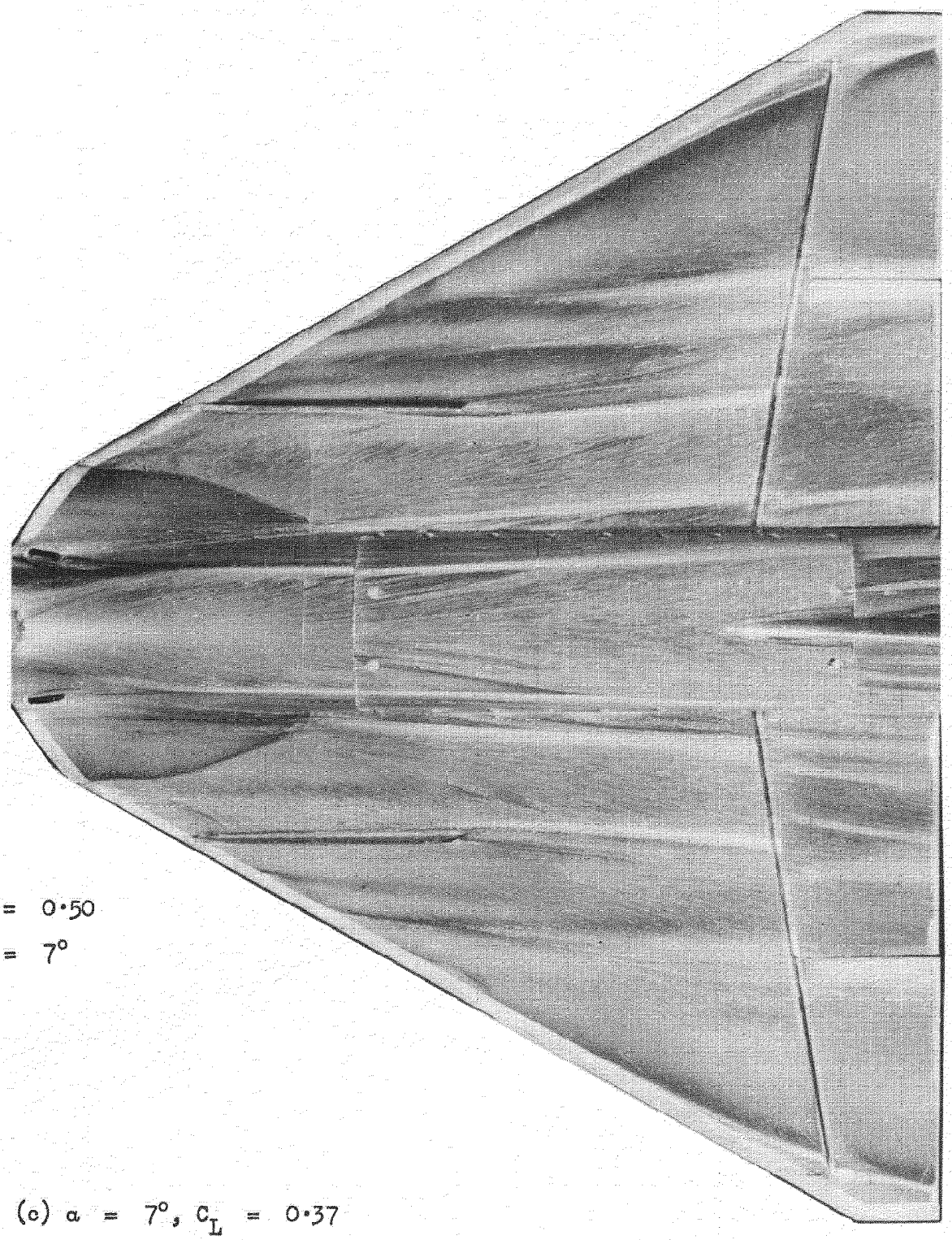

M = 0·50

α = 7°

(c) α = 7°, C_L = 0·37

Fig. 21 Concl'd

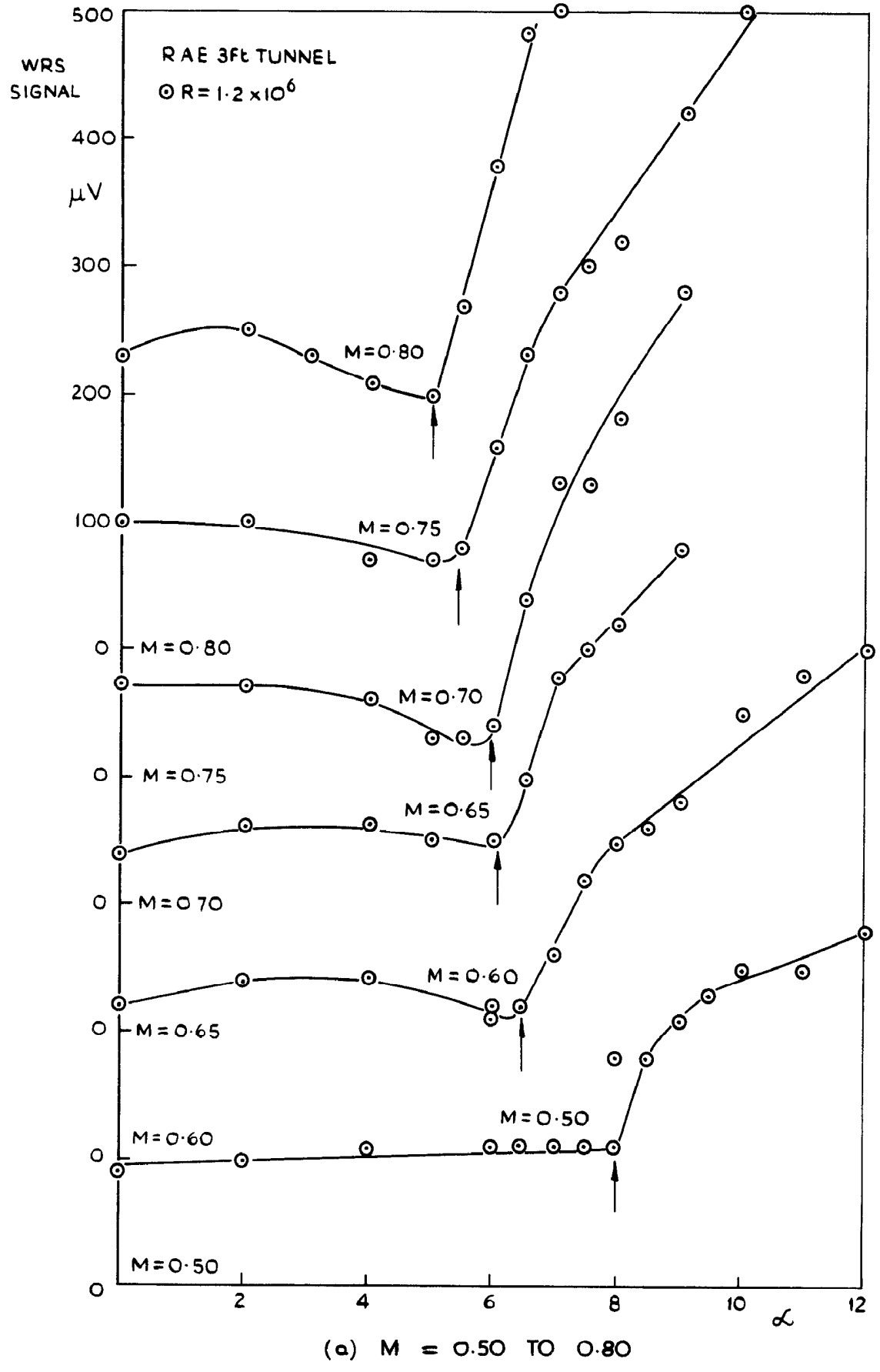

(a) M = 0.50 TO 0.80

FIG. 22 MODEL G - VARIATION OF WING - ROOT STRAIN SIGNAL WITH INCIDENCE.

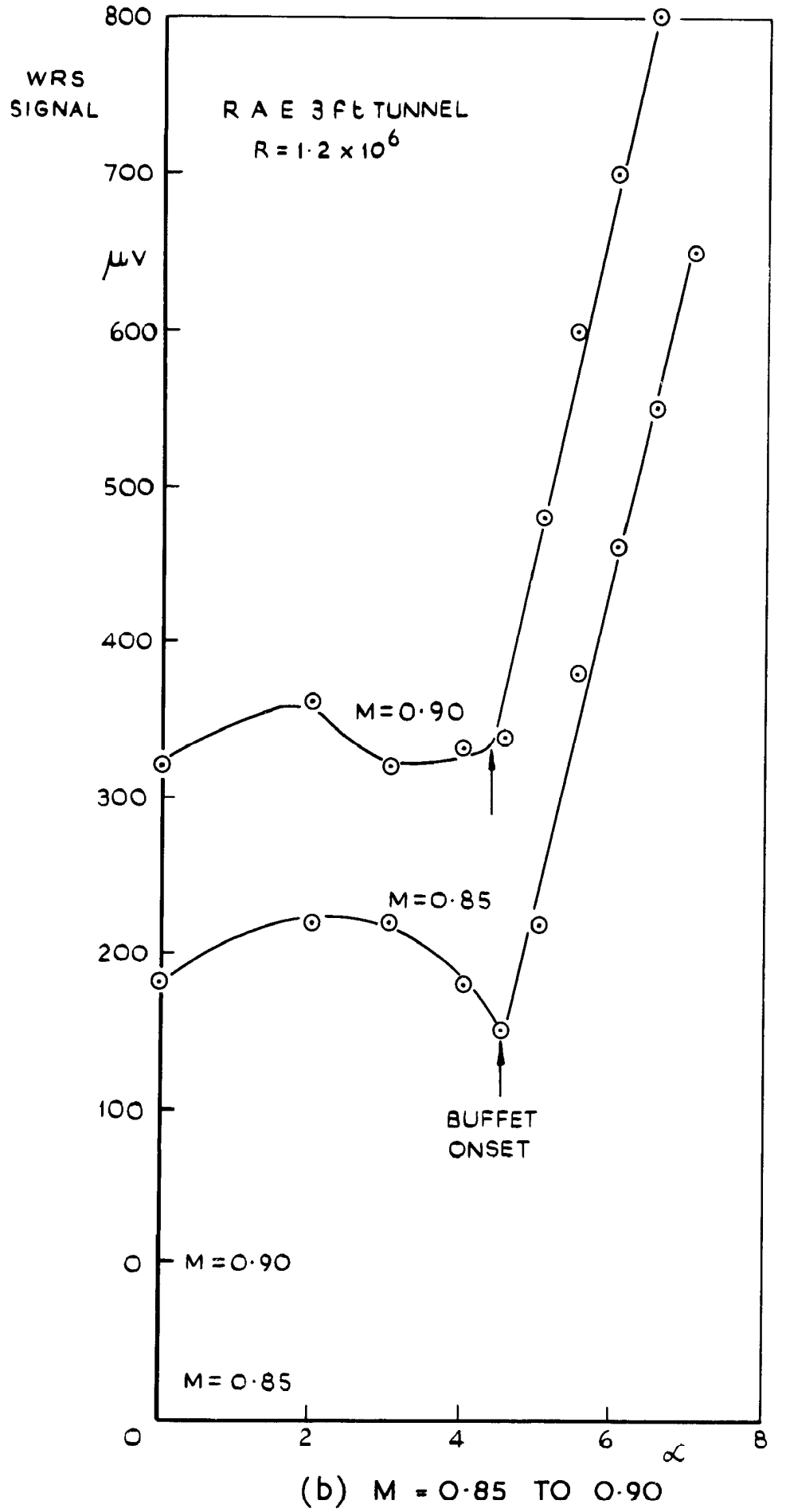

(b) M = 0·85 TO 0·90

FIG. 22 (CONTD)

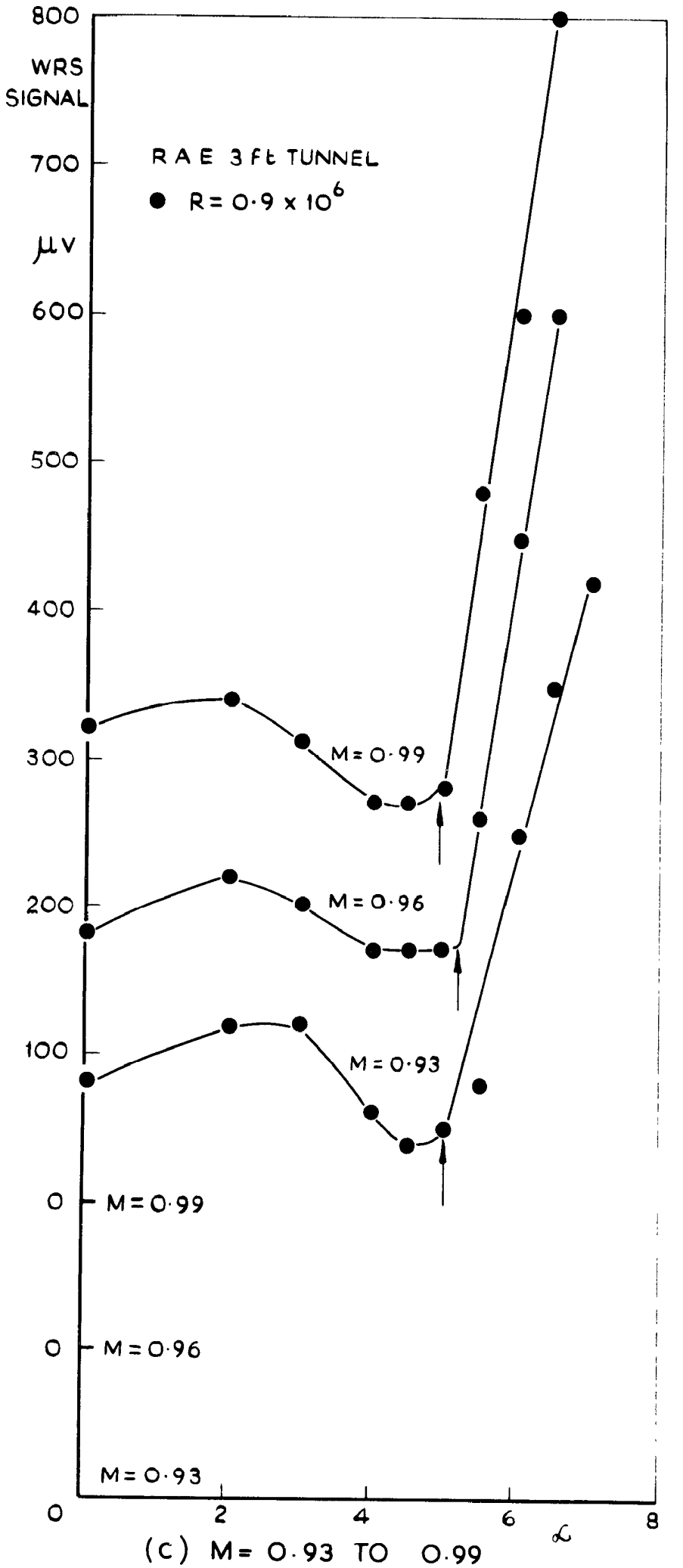

(C) M = 0·93 TO 0·99

FIG. 22 (CONCLD)

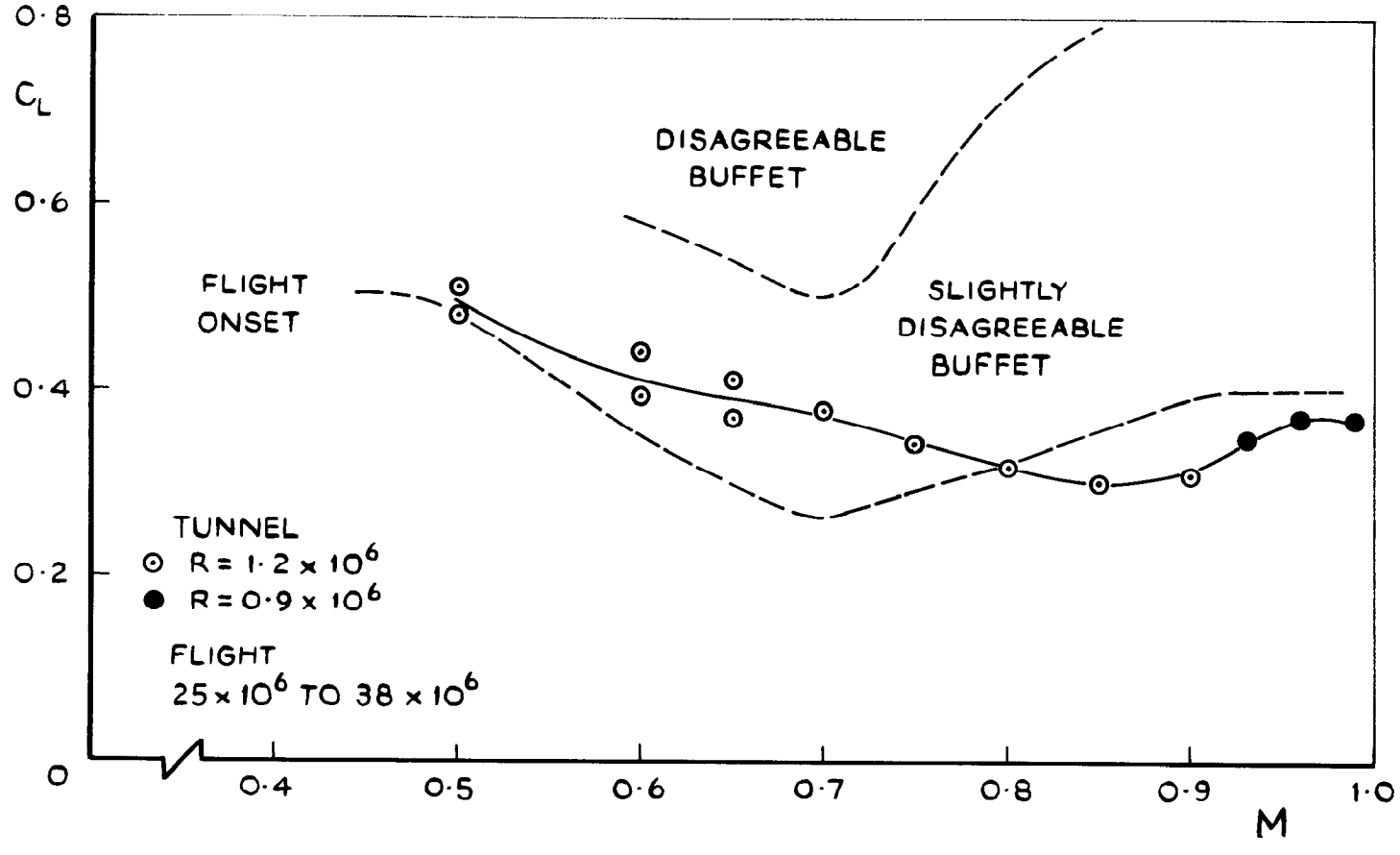

FIG. 23 MODEL G - COMPARISON OF TUNNEL AND FLIGHT BUFFET BOUNDARIES

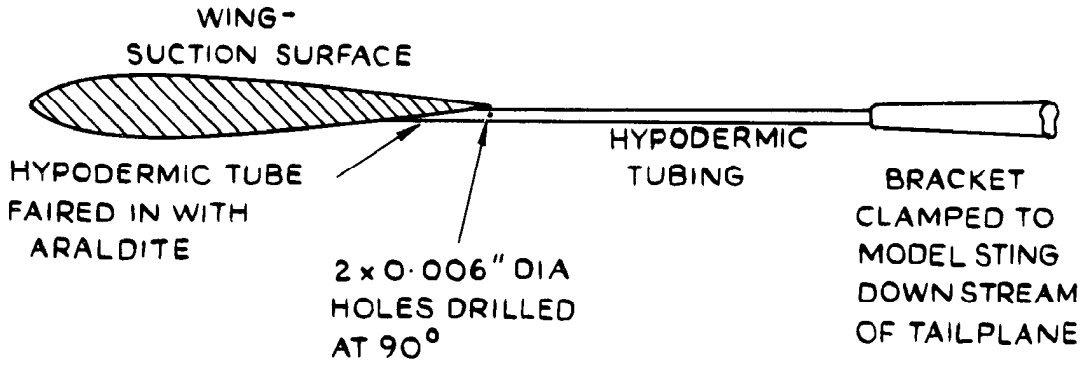

FIG.24 MODEL A - GENERAL ARRANGEMENT OF TRAILING-EDGE STATIC PRESSURE TUBES

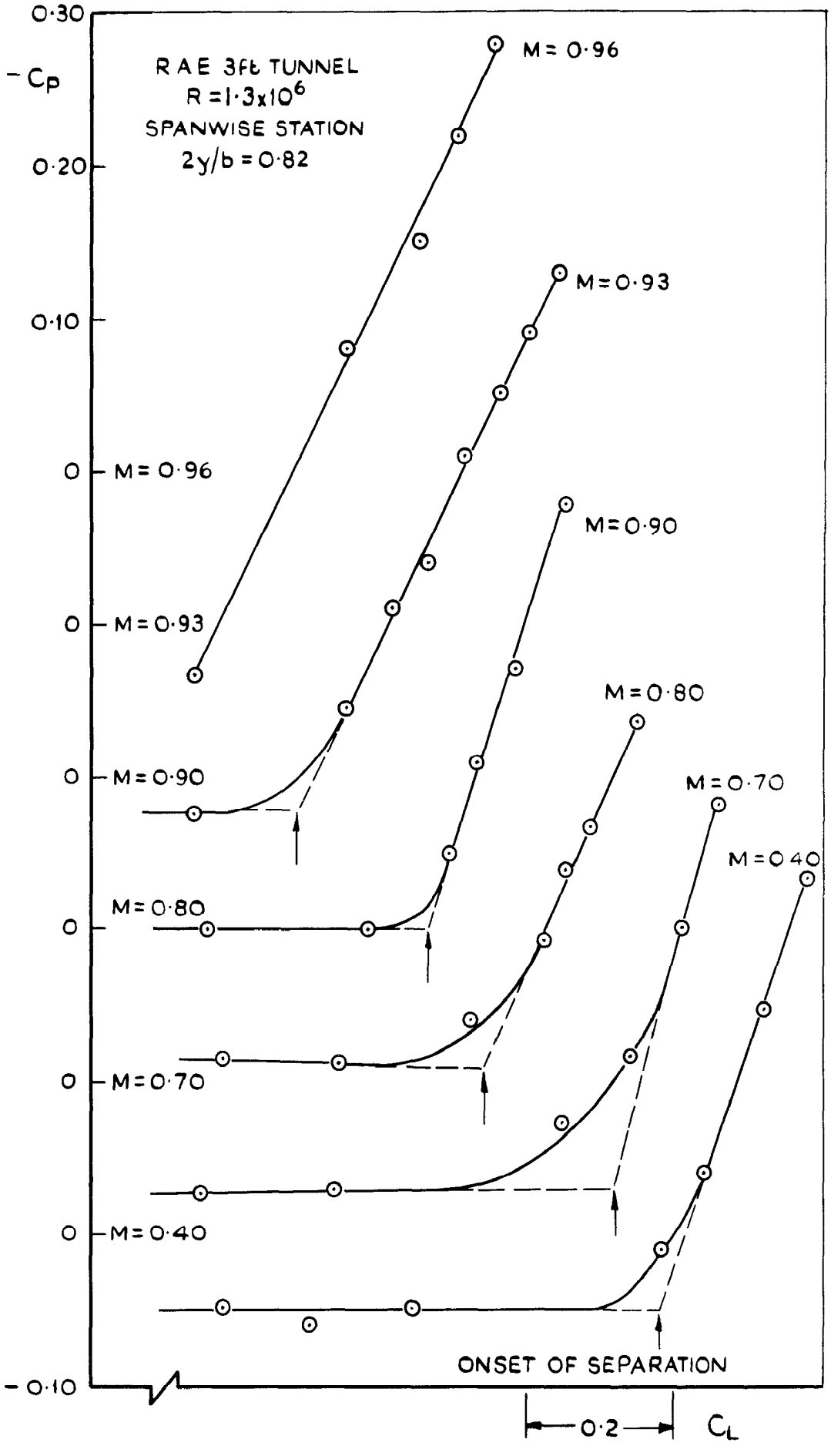

FIG. 25 MODEL A - VARIATION OF TYPICAL TRAILING-EDGE STATIC PRESSURE COEFFICIENT WITH LIFT COEFFICIENT

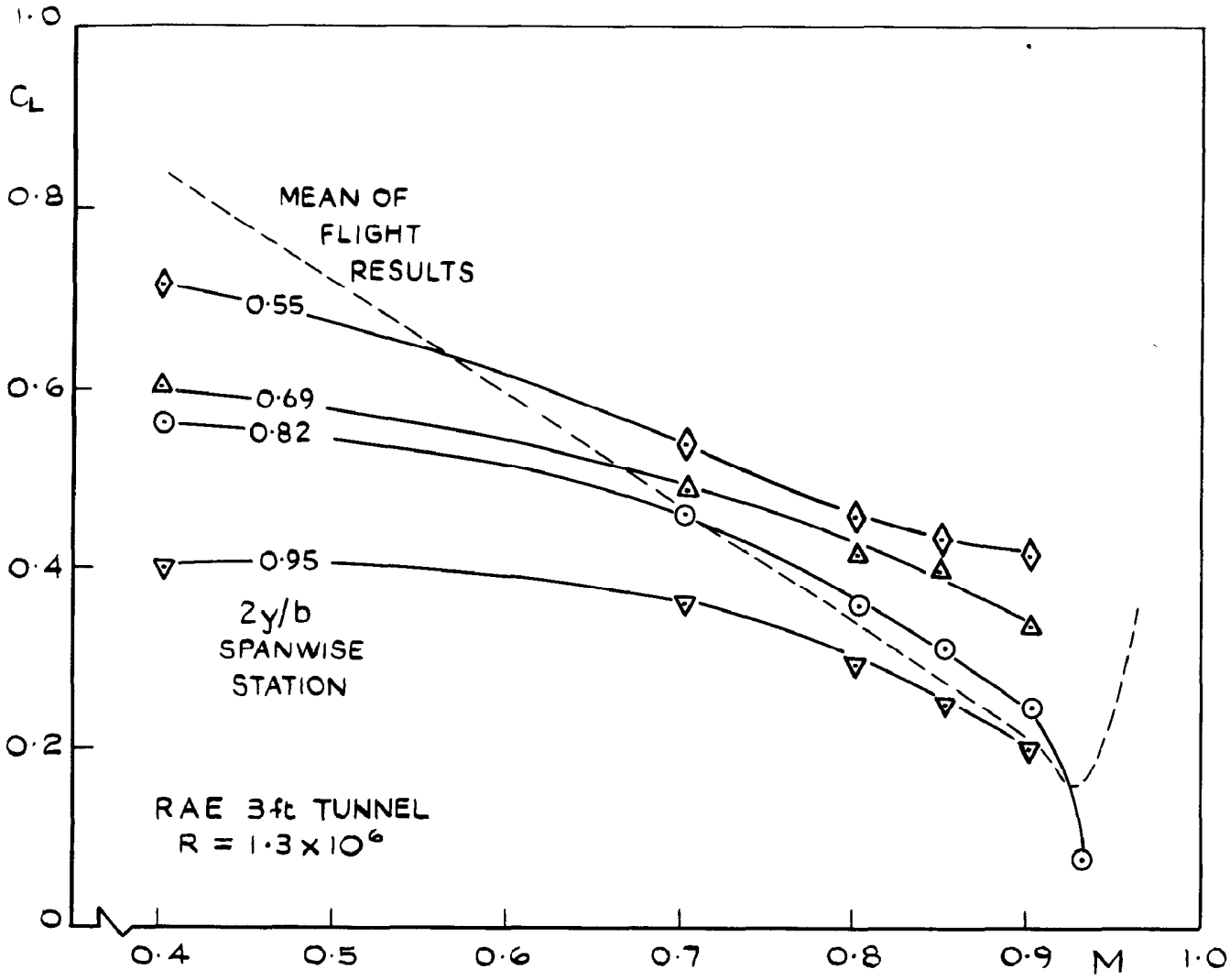

FIG. 26 MODEL A – TRAILING-EDGE STATIC PRESSURE DIVERGENCE BOUNDARIES

Printed in England for Her Majesty's Stationery Office by the Royal Aircraft Establishment, Farnborough. Dd.125875. K.4.

A.R.C. CP No.840

Mabey, D.G.

533.6.013.43 : 533.693

COMPARISON OF SEVEN WING BUFFET BOUNDARIES MEASURED IN WIND TUNNELS AND IN FLIGHT

September 1964

Wing buffet boundaries (for buffet onset) measured on seven wind tunnel models covering an extreme range of planforms are compared with the flight buffet boundaries. The model buffet boundaries are deduced from the variation of fluctuating wing-root strain with incidence at constant Mach number; the flight buffet boundaries are derived from pilot opinion and accelerometer records.

The overall agreement between the tunnel and flight results is fair but there are differences, most of which are probably caused by the low Reynolds number

(Over)

A.R.C. CP No.840

Mabey, D.G.

533.6.013.43 : 533.693

COMPARISON OF SEVEN WING BUFFET BOUNDARIES MEASURED IN WIND TUNNELS AND IN FLIGHT

September 1964

Wing buffet boundaries (for buffet onset) measured on seven wind tunnel models covering an extreme range of planforms are compared with the flight buffet boundaries. The model buffet boundaries are deduced from the variation of fluctuating wing-root strain with incidence at constant Mach number; the flight buffet boundaries are derived from pilot opinion and accelerometer records.

The overall agreement between the tunnel and flight results is fair but there are differences, most of which are probably caused by the low Reynolds number

(Over)

A.R.C. CP No.840

Mabey, D.G.

533.6.013.43 : 533.693

COMPARISON OF SEVEN WING BUFFET BOUNDARIES MEASURED IN WIND TUNNELS AND IN FLIGHT

September 1964

Wing buffet boundaries (for buffet onset) measured on seven wind tunnel models covering an extreme range of planforms are compared with the flight buffet boundaries. The model buffet boundaries are deduced from the variation of fluctuating wing-root strain with incidence at constant Mach number; the flight buffet boundaries are derived from pilot opinion and accelerometer records.

The overall agreement between the tunnel and flight results is fair but there are differences, most of which are probably caused by the low Reynolds number

(Over)

of the tunnel tests. The unsteadiness of slotted tunnels may also influence model buffet over a limited Mach number range.

Future extensions of this dynamic method of buffet measurement on small models are discussed.

of the tunnel tests. The unsteadiness of slotted tunnels may also influence model buffet over a limited Mach number range.

Future extensions of this dynamic method of buffet measurement on small models are discussed.

Published by
HER MAJESTY'S STATIONERY OFFICE

To be purchased from
49 High Holborn, London W.C.1
423 Oxford Street, London W.1
13A Castle Street, Edinburgh 2
109 St. Mary Street, Cardiff
Brazennose Street, Manchester 2
50 Fairfax Street, Bristol 1
35 Smallbrook, Ringway, Birmingham 5
80 Chichester Street, Belfast 1
or through any bookseller

C.P. No. 840

S.O. CODE No. 23-9016-40